WCAP-16996-P, "Realistic LOCA Evaluation Methodology Applied to the Full Spectrum of Break Sizes
(FULL SPECTRUM LOCA Methodology)"
Requests for Additional Information – (Non-Proprietary)
RAIs 46 – 58, 75, and 77

October 2013

Westinghouse Electric Company LLC
1000 Westinghouse Drive
Cranberry Township, PA 16066

Question #46: Containment Pressure Analysis Code COCO Component

The Full Spectrum™ LOCA methodology uses the COCO containment code (Bordelon, F. M., Murphy, E. T., "Containment Pressure Analysis Code (COCO)," WCAP-8327 (Proprietary), WCAP-8306 (Non-Proprietary), 1974) to compute the containment backpressure [

]^{a,c} The COCO code was integrated into WCOBRA/TRAC-TF2. WCAP-16996-P/WCAP-16996-NP, Volumes I, II and III, Revision 0, Section 10.11, "COCO Component," explains that "the COCO computer program (Bordelon and Murphy, 1974) is used to predict the containment pressure response to a LOCA for dry containment buildings, with modeling assumptions to conservatively minimize the back pressure as described in (Bordelon et al., 1974)." WCAP-16996-P/WCAP-16996-NP, Volumes I, II and III, Revision 0, Section 25.6, "Containment Response," further clarifies that COCO is used to calculate the containment pressure [

]^{a,c} Section 25.6 states that input values are shared consistently between WCOBRA/TRAC-TF2 and COCO (i.e., safety injection temperature) with the exception of the single failure assumption. Whereas a failure of a single-train of ECCS is assumed for the LOCA transient calculations, all trains of containment spray, fan coolers, etc. are assumed to be in operation for the containment pressure calculation. Also, Section 25.6 states that "the values for inputs pertinent only to the containment model were typically selected to provide a minimum containment pressure (e.g. maximum heat transfer areas and volumes are modeled for containment heat sinks)." [

]^{a,c}

Please clarify the following items related to the COCO containment component in WCOBRA/TRAC-TF2.

(1) Please identify the frozen code version of the stand-alone COCO containment code that was used to develop the integrated in WCOBRA/TRAC-TF2 and provide a complete set of references that document this code version. Explain if this code version has been approved by the U.S. Nuclear Regulatory Commission (NRC) and provide appropriate references. If any changes were made to the stand-alone code as part of its integration in to WCOBRA/TRAC-TF2, please describe these changes and explain if they have been previously reviewed and approved by NRC.

(2) Please describe briefly the balance equations used in the lumped parameter modeling approach and identify the subsystems included in the containment model. In addition, describe the implemented modeling assumptions and explain any possible non-conservatism in the modeling approach. Describe the modeling of engineered features, components and safety systems that can have an impact on the containment pressure response predictions and identify any modeling limitations in this regard.

(3) Please describe and present results from validation cases that demonstrate the applicability and appropriateness of the COCO component for the purposes of the FULL SPECTRUM™ LOCA methodology. Identify any modeling biases and their possible impact on LBLOCA prediction results.

(4) COCO is used to calculate the temperature and pressure inside a pressurized water reactor (PWR) dry containment following a LOCA for containment design (i.e., peak pressure) as well as for containment backpressure prediction for LOCA analyses. Please identify and provide a list of all parameters for which Section 25.6 states that "the values for inputs pertinent only to the containment model were typically selected to provide a minimum containment pressure" applies. In addition, please provide these selected values and explain the basis for their determination. Clarify if any of these input values are plant-specific and if so explain how it is ensured that appropriate inputs will be used for intended FULL SPECTRUM™ LOCA methodology applications.

(5) Please describe the modeling options for determining the heat transfer to containment walls and structures (e.g., input tables). Please describe any implemented heat transfer coefficient correlations along with their range of applicability and activation logic. Explain how [

]^{a,c} was determined and implemented in the COCO component.

(6) Please identify any parameters related to the COCO component that are subject to sampling in FULL SPECTRUM™ LOCA methodology applications. For each such parameter, define the sampling range and distribution and explain their determination for best-estimate plant LOCA applications.

(7) WCAP-16996-P/WCAP-16996-NP, Volumes I, II and III, Revision 0, Section 10.11, "COCO Component," refers at its end to topical report Section 25.5, "Operator Actions." It is believed that the reference in Section 10.11 should be to Section 25.6, "Containment Response," instead of Section 25.5, "Operator Actions."

Response:

Response to Question 1

The frozen code version of the stand-alone COCO version used to develop the integrated WCOBRA/TRAC-TF2 model is COCO_A Version 1.4, which was built using COCOLIB.A Version 1.2. The references that document this code version are WCAP-8327-P (Reference 1), Containment Pressure Analysis Code (COCO), and WCAP-8339 (Reference 8), Westinghouse Emergency Core Cooling System Evaluation Model. Reference 1 provides the code description and Appendix A of Reference 8 provides instructions as to how the code will be applied.

COCO was approved by the NRC as part of the LOCA 1975 Evaluation Model according to WCAP-8471-P-A (Reference 3), which references the COCO topical report (Reference 1). This COCO topical was also referenced in the BASH Evaluation Model in WCAP-10266-P-A (Reference 5). According to the SER, Section 3.5, Item I.D.2 in Reference 5, "The COCO and LOTIC codes are used in the same manner as previously approved by the NRC. Pressure reducing effects are maximized." Also, according to Section 6.4 of Reference 5, "COCO is accepted for ECCS calculations and is described in detail in WCAP-8327." In addition, page 2-8 of WCAP-9220-P-A, Revision 1 (Reference

4), specifies that paint may be modeled on the containment walls in the COCO code. This change was approved as part of the 1978 and 1981 versions of the Westinghouse ECCS Evaluation Models in Reference 4.

There are several changes made to the stand-alone code as part of its integration in WCOBRA/TRAC-TF2, which include the following:

a) Coupling logic / Time-Step Treatment: The containment conditions are updated after each WC/T-TF2 time-step. In this case, COCO will use the mass and energy releases (M+Es) at the end of each successful WC/T-TF2 time-step as boundary conditions at the BREAK until the COCO calculations catch up to the WC/T-TF2 time-step. In most cases, COCO will need only one time-step to catch up, since the WC/T-TF2 time-step size is typically small compared to the typical COCO time-step size.

b) Treatment of boundary conditions: COCO and WC/T-TF2 have been integrated to pass boundary condition information back and forth at each WC/T-TF2 time-step. This allows every break case to have immediate feedback with the containment, and allows each WC/T-TF2 run to have different containment pressure boundary conditions. There is no impact on the WC/T-TF2 solution matrix or numerical solution method as a result of this difference because the data is transferred as boundary conditions from the last time-step of one code feeding the new time-step of the other code.

In order to pass the boundary condition information between COCO and WC/T-TF2 at each time-step, the COCO "Air Addition" and "Steam – Air Removal" capabilities are used as the path to provide flow of non-condensable gases (NCD) from WC/T-TF2 to containment (Air Addition), and the path to supply steam and/or NCD from containment back to WC/T-TF2 (Steam – Air Removal). Therefore, the changes to COCO only involve provision for the new boundary conditions with WC/T-TF2 and do not represent a change to the numerical solution of COCO. At the end of each WC/T-TF2 time-step, the following boundary conditions are provided to COCO: [
]^{a,c} In addition, COCO provides the following boundary conditions back to WC/T-TF2 for its next time step: [
]^{a,c}

In order for WC/T-TF2 to interface with COCO, a new type of BREAK component is used to pass the boundary conditions between the codes. For a typical plant analysis, one BREAK would be needed for split breaks, and two for double-ended guillotine (DEG) breaks. Using the COCO containment conditions as a boundary condition means that there are no changes required to the WC/T-TF2 solution matrix, or numerics, and only the source and input of the BREAKs are modified.

c) Change in treatment of non-condensable gases: According to page 2-3 of Reference 1, COCO has capabilities for modeling two NCD gases. One of the changes to the code is to pass non-condensable gas information between WC/T-TF2 and COCO at the BREAK interface. With the addition of a NCD in the TRAC PF1 components and the COBRA VESSEL component, changes are needed as follows;

- WC/T-TF2 must provide the NCD M+Es to COCO and accept the revised containment NCD conditions from COCO

- COCO must accept and use the NCD M+Es and pass the containment NCD conditions back to WC/T-TF2

As part of this change, it is necessary that flows from the containment to WC/T-TF2 are modeled. Thus, if WC/T-TF2 predicts flows from containment into the BREAK, COCO must recognize this condition and treat these flows appropriately. For flows from the BREAK to the containment, COCO accepts 2-phase mixture M+Es and separate NCD M+Es. For flows from the containment to the BREAK, only steam and NCD M+Es are considered, since the liquid modeled by COCO is only in the sump, with no communication path to the BREAK.

d) Input changes are described in further detail in responses to Questions 4, 5, and 6. Specifically, there are changes to the safety injection water temperature and delay time inputs (see Question 6), the end-of-blowdown time and blowdown energy inputs (see Question 5), and a few other input updates due to the coupling of COCO and WC/T-TF2 (see Question 4).

These changes have not been previously reviewed and approved by the NRC, but are not considered significant changes to the code itself. The COCO-interface in WC/T-TF2 is behaving consistent with the stand-alone COCO_A Version 1.4 computer program.

Response to Question 2

COCO uses continuity and energy equations in a lumped parameter modeling approach as described in Section 2.2 of Reference 1. In addition, COCO uses volume equations, equations of state, and steam and water tables. The energy equations used for modeling the containment walls are described in Section 2.3 of Reference 1 and are discussed in more detail in the response to Question 5. The auxiliary systems in the containment model are described in Section 2.4 of Reference 1, and include flashing of break flow, heat sources, and venting. Modeling assumptions a) through d) are described in Section 2.1 of Reference 1, and include the following:

a) The containment air-steam-water mixture is separated into two distinct systems. The first system is the air-steam phase, while the second is the water phase in the containment sump. COCO assumes uniform thermodynamic conditions in each of these systems, but this does not imply continual thermal equilibrium between the air-steam mixture and the water phase. COCO uses the fundamental laws of thermodynamics to solve for the containment conditions at any time.

b) Air inside containment is treated as an ideal gas. The thermodynamic properties of steam as found in the 1967 ASME steam tables adopted by the Sixth International Conference on the Properties of Steam are used in COCO.

c) For heat transfer through and heat storage in walls of the containment structure, only multi-layered flat walls are considered and heat transfer is neglected in any direction perpendicular to the wall surface. In addition, the thermal conductivity, density and specific heat of each heat layer are assumed to be constant.

d) Two phase discharge flow is divided by assuming the liquid part to be saturated liquid at the total containment pressure, and the steam part to be saturated vapor at the steam partial pressure in the containment. For single discharge flow, the flow goes directly to the appropriate system.

It is noted that these four assumptions have always existed in the containment modeling approach, and originated in the as-approved COCO version. The changes to COCO as a result of coupling WC/T-TF2 and COCO are described in response to Question 1, and are considered modeling implementation approaches rather than modeling assumptions. As discussed in response to Question 6, the safety injection temperature and delay times are input to COCO [

]^{a,c}

The engineered features, components and safety systems included in the COCO containment code are described in Section 2.5 of Reference 1, and are described in more detail in response to Question 4. The engineered safeguards modeled in COCO are containment ventilation fan coolers, internal spray system, recirculation cooling system, and external spray.

Response to Question 3

Section 3 of Reference 1 presents a validation case comparing the COCO code prediction to experimental test data. The COCO code performance was shown to be in good agreement with the corrected test temperatures from the work of Kolflat and Chittenden (Reference 6). In addition, the code was compared to other techniques including the CONTEMPT code, which is an independently derived containment analysis code used by the (former) Atomic Energy Commission (AEC) staff. The response to Question 1 shows that the COCO version in Reference 1 is very similar to the coupled COCO version in WC/T-TF2. Therefore, the results of this validation case still remain applicable to the COCO Version 1.4 used with WC/T-TF2.

To validate the coupled WC/T-TF2 and COCO code Version 1.4, several validation test cases were performed to ensure the implemented features were functioning as intended. In addition, the standalone COCO containment pressure calculations were compared with WC/T-TF2 coupled run calculations. The following validation test cases were performed:

a. [

b.

]^{a,c}

c. [

d.

          ]^{a,c}

Modeling biases in the COCO inputs are typically selected to conservatively minimize containment backpressure from a LOCA perspective. See the response to Question 4 for the parameters that are typically selected to provide a minimum containment pressure, and see the response to Question 5 for further information on the [   ]^{a,c}

Response to Question 4

The COCO input parameters were reviewed to identify those that are intentionally selected to provide a minimum containment pressure.

COCO Inputs

- The standard COCO break flow model input results in break flow flashing into steam at steam partial pressure and water at total containment pressure. All of the steam from the break goes to the atmosphere, and all of the water from the break goes to the sump.

- Several inputs are used for coefficients and multipliers in the Tagami correlation.

   o As discussed in Appendix A, Section III.B.1 of Reference 8, the maximum condensing heat transfer coefficient at the end of blowdown is five times higher than that calculated using the Tagami correlation.

   o As discussed in Appendix A, Section III.B.3 of Reference 8, in the post-blowdown period of the transient, the coefficient for exponential decay in the Tagami correlation is specified as 0.05.

- The [

                         ]^{a,c} respectively. These inputs are discussed further in the
response to Question 5.

- The net free volume of containment is a plant-specific input, and is biased high to minimize containment backpressure.

- The initial state of containment has four possible modeling options, which are described in Section 2.2 of Reference 1. According to page 2-3 of Reference 1, the condition of superheated steam and subcooled water is intended to represent the containment atmosphere in the form of air with a small relative humidity. This condition is typically used for LOCA applications of COCO.

- <u>Containment Passive Heat Sinks</u>

  - o The containment heat sink inputs are developed from plant-specific data. The surface area, thickness, and materials of each layer present (including paint), as well as the thermal conductivity, and volumetric heat capacity of each material is requested. Maximum values are conservative for all areas, thicknesses, etc, with the exception of paint layer thickness. A minimum value is conservative for paint layer thickness. Also, for thermal conductivity and specific heat, the maximum values are recommended for use. See the response to Question 5 for additional information about the heat sink modeling approach.

  - o COCO has the capability to specify the heat transfer boundary condition at the outer surface of each layer of the walls. Options include specifying a constant heat transfer coefficient, modeling the outer surface of the layer of the wall as adiabatic, or inputting the surface emissivity for radiation heat transfer. Standard LOCA values for the various surfaces modeled in COCO include the following:

    - Heat transfer coefficient for steel/concrete interfaces of 300 BTU/hr-ft^2-°F. According to pages A-3 and A-4 of Reference 8, preliminary results of experimental data show that the coefficient lies in the range of 10-100 BTU/hr-ft^2-°F, but 300 BTU/hr-ft^2-°F is used as a conservatively bounding value.

    - Heat transfer coefficient for paint/paint, paint/steel, paint/concrete, and concrete/concrete interfaces of [

      ]^{a,c} Therefore, the heat is able to flow through the paint layers, and is stored in the interior layers of the wall.

    - For the final layer of an internal wall, adiabatic conditions are modeled.

    - For the external surface of the containment building exposed to the atmosphere, an emissivity of [   ]^{a,c} is modeled. According to Table A.11 of Reference 10, the emissivity of concrete is between 0.88 and 0.93, thus [   ]^{a,c} is an adequate representative value for the emissivity of concrete.

- <u>Initial Conditions</u>

  - COCO provides two options for the user to specify initial containment parameters. The first is to input initial containment parameters for water and steam (and then the code specifies or calculates the other initial conditions), or the initial conditions can be specified for air, hydrogen, steam, and water. In a typical LOCA analysis, the latter option is used with the following initial conditions specified for each biased to minimize the calculated containment pressure:

    - Initial pressures are set by the user for air, hydrogen, steam, and water. The initial containment pressure for LOCA evaluation models has typically been set to [

      ]^{a,c} The initial water pressure is set to the initial containment pressure. The partial pressures for steam and air are then calculated using the initial containment pressure and the initial containment temperature, conservatively assuming [   ]^{a,c} relative humidity. Finally, the initial hydrogen pressure is set to zero. The generic value of [   ]^{a,c} is justified in ET-NRC-92-3699 (Reference 9).

    - Gas constant and specific heat are set by the user for air and hydrogen only. Standard gas constants of 53.3 ft-lbf/lbm-°R and 767 ft-lbf/lbm-°R are used for air and hydrogen, respectively. Standard specific heats of 0.24 BTU/lbm-°F and 3.42 BTU/lbm-°F are used for air and hydrogen, respectively.

    - Initial temperatures are set by the user for steam and water only. The initial containment temperature for LOCA evaluation models has typically been set to [   ]^{a,c} for dry-atmospheric containments. This value is further justified in Reference 9.

- <u>Fan Coolers</u>

  - [

    ]^{a,c} is a plant-specific input which is biased high in the COCO code. For a plant with fan coolers, the utility is recommended to specify [

    ]^{a,c} It is noted that if there are no fan coolers in the plant design, none are modeled.

  - The minimum fan cooler initiation delay time is [

    ]^{a,c} For FSLOCA applications, [

    ]^{a,c} This is noted as a departure from prior COCO applications where the delay time was [

    ]^{a,c}

o The heat removal rate is [

]^{a,c}

- **Recirculation Modeling**

    o This set of inputs is used to enter information related to recirculation modeling, which is used for plants with [   ]^{a,c} and plants with [

]^{a,c}

    o The recirculation modeling approach has not changed as a result of coupling COCO and WC/T-TF2; therefore, the recirculation cooling system described in Section 2.5.3 of Reference 1 is still applicable.

    o The plant provides the minimum recirculation spray pump initiation time, and the delay time is [   ]^{a,c} For FSLOCA applications, [

]^{a,c} This is noted as a departure from prior COCO applications where the delay time was [   ]^{a,c} If the plant is not equipped with a recirculation containment spray system that can operate during ECC injection mode coincident with the containment spray system, or if the recirculation spray system only initiates after the large break LOCA transient has ended, then this input is not required. However, if the recirculation pumps come on before the LOCA transient has ended, then additional plant-specific inputs will be requested from the plant.

- **Internal Spray**

    o The maximum containment spray flow rate [   ]^{a,c} is a plant-specific input. [

]^{a,c}

    o The containment spray start time (spray pump initiation delay) is [
]^{a,c} For FSLOCA applications, [

]^{a,c}
This is noted as a departure from prior COCO applications where the delay time was [
]^{a,c} The containment spray stop time is

typically entered as a value much greater than the transient end time to ensure continuous spray flow throughout the entire transient.

o   The containment spray temperature input is [   ]a,c in the FSLOCA applications. The SI spray temperature will be modeled [
                              ]a,c It is noted that this is a change from prior applications, where this input was typically taken as the [
                              ]a,c

o   In a typical LBLOCA analysis, the spray inputs are used to model the [

]a,c

- **Wall Surface Heat Transfer Coefficient vs. Time Tables**

    o   COCO has the capability to model a table of wall surface heat transfer coefficients vs. time. It is recommended that the inside surface film heat transfer coefficient is equal to [   ]a,c at all times. This generic coefficient value is generally used for walls in contact with the containment sump. This parameter is not expected to have much influence on the containment pressure calculation for FSLOCA, though it is assumed to be sufficiently high to adequately remove heat from the sump.

- **Air Addition Input Capabilities**

    o   A table of air addition mass flow rate and temperature vs. time can be input to COCO. The table contains values of [

]a,c Note that the air addition table is used to model the emptying of the broken loop accumulator. Transport of the NCD gases from the intact loop accumulators is modeled in WC/T-TF2. When it travels through the RCS to the break, it is introduced to the COCO calculation.

Response to Question 5

The heat transfer to containment walls and structures is described in Section 2.7.2 of Reference 1. The modeling options to determine the heat transfer to the containment walls and structures have not changed as a result of integrating COCO in WC/T-TF2. Overall, the code has the capability to model [   ]^{a,c} which was a minor change implemented into COCO_A, Version 1.4. Structural heat sinks are modeled as a series of layers, and there can be up to a maximum of [   ]^{a,c} layers per heat sink. For each heat sink [

                                                    ]^{a,c} is input. In addition, the analyst can specify the method for calculating the wall heat transfer coefficient for structural heat sinks, and whether the heat sink is in contact with the sump or steam-air mixture. For the wall heat transfer coefficient, in a typical plant analysis, the Tagami Correlation for heat transfer to steel or to concrete is used, depending on the material of the structural heat sink. These coefficients are calculated internally. In addition, the code has the capability for time or temperature dependent user-specified heat transfer coefficient tables. Then, for each of the layers for all heat sinks, the thickness of the layer, the thermal conductivity, the volumetric heat capacity, and the heat transfer boundary condition at the outer surface of the layer is modeled.

COCO uses the Tagami correlation to describe the heat transfer coefficients between the containment atmosphere and the containment structures. To use the Tagami correlation in COCO, the time from the start of accident to the end of blowdown must be input. In addition, the coolant energy discharged from the beginning of the accident until the end of blowdown must be specified. For the FSLOCA application of COCO, [

                                                                                            ]^{a,c}

According to Equation 56 of Reference 1, the maximum heat transfer coefficient is proportional to the blowdown energy raised to a power of 0.6, and inversely proportional to the end-of-blowdown time raised to a power of 0.6. Therefore, minimizing the end-of-blowdown time and maximizing the blowdown energy will maximize the heat transfer coefficient, and minimize the calculated containment pressure. [

                            ]^{a,c}

The Demonstration Analysis, presented in Section 31 of Reference 7, used [

]^{a,c} which was shown to be bounding for the Demonstration Analysis.

Response to Question 6

The response to RAI 77 describes the sampled parameters in an FSLOCA uncertainty analysis. These parameters were examined to determine which, if any, are also used as inputs in the LOCA containment pressure calculations. Based on a review of Table 1 of the response to RAI 77, [

]^{a,c}

For a plant-specific application of FSLOCA, the [
                    ]^{a,c} are determined by input from the plant. The sampling range is based on historical data provided by the plant per Table 29-5 of Reference 7. RAI 77 provides additional information regarding the [   ]^{a,c}

In addition, there are other sampled parameters that have an impact on the containment response during a LOCA. Due to the implementation of coupling WCT-TF2 and COCO, the break M+Es are passed between the two codes during the transient. As a result, the break type, break area, and discharge coefficients are sampled parameters which indirectly influence the containment backpressure calculation as the size of the break will impact on the M+Es that are released to containment. It is noted that all of the sampled parameters in FSLOCA may indirectly have a minor impact on the containment backpressure calculation during a LOCA.

Response to Question 7

Westinghouse agrees with the observations noted in Question 7. Revisions to correct cross references will be made as part of the overall topical report updates.

References:

1. **WCAP-8327-P**, "Containment Pressure Analysis Code (COCO)," July 1974 (*Note that the non-proprietary version is available as WCAP-8326-NP).*

2. Not used.

3. **WCAP-8471-P-A**, "THE WESTINGHOUSE ECCS EVALUATION MODEL: SUPPLEMENTARY INFORMATION," April 1975.

4. **WCAP-9220-P-A, Revision 1**, "WESTINGHOUSE ECCS EVALUATION MODEL 1981 VERSION," February 1982.

5. **WCAP-10266-P-A, Revision 2**, "The 1981 Version of the Westinghouse ECCS Evaluation Model Using the BASH Code," March 1987.

6. **Kolflat, A., and Chittenden, W.**, "A New Approach to the Design of Containment Shells for Atomic Power Plants," Proceedings of American Power Conference, pg. 651, Vol. XIX, 1957.

7. **WCAP-16996-P, Volumes I through III**, "Realistic LOCA Evaluation Methodology Applied to the Full Spectrum of Break Sizes (FULL SPECTRUM LOCA Methodology)," November 2010.

8. **WCAP-8339**, "Westinghouse Emergency Core Cooling System Evaluation Model Summary," June 1974.

9. **ET-NRC-92-3699**, "Results of Technical Evaluation of Containment Initial Temperature Assumptions for Large Break Loss of Coolant Accident Analysis," June 1, 1992.

10. **Incropera, F. P., DeWitt, D. P., Bergman, T. L., and Lavine, A. S.**, "Fundamentals of Heat and Mass Transfer," Sixth Edition, John Wiley and Sons, 2007.

Question #47: TRAC-PF1 One-Dimensional Component Models

WCAP-16996-P/WCAP-16996-NP, Volumes I, II and III, Revision 0, Section 10, "WCOBRA/TRAC-TF2 One-Dimensional Component Models," explains that the one-dimensional components in WCOBRA/TRAC-TF2 used to model the reactor primary system are derived from TRAC-PF1. As stated in Subsection 10.1, "Introduction,"

> "many of the base modules, such as PIPE, TEE, HTSTR, VALVE
> and PUMP are virtually unchanged from their original TRAC-PF1
> versions, so their descriptions are very similar to those given by
> TRAC-PF1 user manual."

Please clarify the following items related to the one-dimensional component modules in WCOBRA/TRAC-TF2.

(1) Please identify the frozen code version of TRAC-PF1, from which the one-dimensional component modules implemented in WCOBRA/TRAC-TF2 were taken and provide a reference to the cited TRAC-PF1 user manual. In addition, explain how it was determined that the existing TRAC-PF1 modules were adequate for the purposes of the WCOBRA/TRAC-TF2 code. If any changes were made to these modules as part of their integration in WCOBRA/TRAC-TF2, please document the changes and explain if they have been previously reviewed by NRC.

(2) In describing the HTSTR component, WCAP-16996-P/WCAP-16996-NP, Volumes I, II and III, Revision 0, Subsection 10.10, "HTSTR Components," refers on several occasions to the TRAC-M code. TRAC-M was the predecessor of the TRACE code developed by the NRC. Please identify the code from which the HTSTR component was taken and explain how TRAC-M was used for the purpose of implementing this HTSTR component in WCOBRA/TRAC-TF2.

Response:

Text references to TRAC-M, TRAC-P, TRAC-PF1, or TRAC-PF1/MOD2 represent the same base (frozen) TRAC code version: TRAC-P Version 5.4.28. WCAP-16996-P/WCAP-16996-NP will be updated to replace the aforementioned code version references with a single TRAC-P code reference, which is TRAC-P Version 5.4.28. However, actual referenced documents may still point to other TRAC versions when they represent the best known available information.

TRAC-P Version 5.4.28 is the frozen version transmitted to Westinghouse by the USNRC via Information Systems Laboratories with the following letter:

ISL-TRAC-04-002   "TRAC-04-002: Transmittal of TRAC-P Version 5.4.28,"
September 2004.

The user manual cited for this frozen version is the following:

LA-UR-00-834   "TRAC-M/Fortran 90 (Version 3.0) User's Manual,"
                      Steinke, R. G., et al., February 2000.

The following are the other references identified as documentation of the frozen version:

LA-UR-99-2312   "TRAC-M/Fortran 77, Version 5.5, Programmer's Guide,"
                      Steinke, R. G., et al., October 1999.

LA-UR-00-803   "TRAC-M/Fortran 90 (Version 3.0) Programmer's Manual,"
                      Adams, B. T., et al., February 2000.

LA-UR-00-910   "TRAC-M/Fortran 90 (Version 3.0) Theory Manual," Spore, J. W., et al.,
                      July 2000.

LA-UR-01-2105(1)   "TRAC-M/F77, Version 5.5, Developmental Assessment Manual,
                      Volume 1: Assessments, " Boyack, B. E., et al., April 2001.

LA-UR-01-2105(2)   "TRAC-M/F77, Version 5.5, Developmental Assessment Manual,
                      Volume 2: Appendices," Boyack, B. E., et al., April 2001.

The TRAC-PF1/MOD2 code version (TRAC-P) was considered to be mature for the purpose of WCOBRA/TRAC-TF2 (WCT-TF2) development. It was the final TRAC code version available in a format compatible with the Fortran 77 structure of the WCOBRA/TRAC (WC/T) code in use at Westinghouse for predicting the response of a pressurized water reactor (PWR) to a loss of coolant accident (LOCA), and it provided additional capabilities not present in WC/T, based on the TRAC-M Theory Manual (Spore, et al., 2000) and TRAC-M Assessment Manual (Boyack, et al., 2001).

WC/T was previously qualified for the realistic analysis of PWR Large Break (LB) LOCAs. TRAC-P provided additional capabilities to potentially expand the application of WC/T to the full spectrum of breaks: small, intermediate, and large. The TRAC-P 1D module provided enhanced LBLOCA features (e.g. non-condensable gas transport) and added capabilities to properly capture the important processes and phenomena identified for small and intermediate break scenarios. It featured expanded fundamental field equations and closure relationship models which are essential to extend the WC/T code capabilities. The TRAC-P six-equation two-fluid solution provides adequate formulation for horizontally stratified flow simulation required for Small Break (SB) LOCA analysis, in comparison to the formulation in WC/T (which is based on TRAC-PD2).

The TRAC-P developmental assessment documentation (Boyack, et al., 2001) demonstrated that TRAC-P was a viable tool for analyzing PWRs during a LOCA and other operational transients, by successful comparisons to analytical solutions, separate effect tests, and integral effect tests.

The adequacy of the WCT-TF2 individual 1D-components has been demonstrated by performing successful comparisons to analytical solutions, separate effect tests, and integral effect tests, as provided in WCAP-16996-P/WCAP-16996-NP.

Changes to 1D-Components

The following summarizes the source code changes made to the TRAC-P 1D-components during the development of the WCT-TF2 code, and identifies specific WCAP-16996-P/WCAP-16996-NP section numbers where each change is described and/or assessed, when appropriate:

1.   **Generic** No further documentation in WCAP-16996-P/WCAP-16996-NP for these changes, unless noted.

    a. Ported program to GNU Linux, using Intel Fortran (ifort).

    b. Added and improved input checking logic for all 1D-components to consistently provide an ERROR or WARNING message when appropriate. Corrected and improved output information related to input.

    c. [

        ]^{a,c} is described in Section 5.12, and demonstrated in Section 12.0.

    d. [   ]^{a,c}

2.   **BREAK** See Section 10.9 and Section 10.11.

    a. Added IBTY=101 option to interface with COCO for containment boundary conditions. Up to [   ]^{a,c} BREAK components can interface with COCO.

3.   **FILL**   See Section 10.9. No FILL-specific changes.

4.   **HTSTR** See Section 10.10 for HTSTR description, and Section 10.5 for use of HTSTR in steam generator model. No HTSTR-specific changes.

5.   **PIPE**   See Section 10.2.

    a. Added [

        ]^{a,c} applied in TF1D.

    b. Added [

        ]^{a,c} applied in PREPER.

    c. Modified flow regime map (and use of inputs [   ]^{a,c}). Horizontal stratification in a PIPE can be controlled by [   ]^{a,c} input. Calculations in FEMOM and HTIF. See Section 4.4.

6.   **PRIZER** See Section 10.6.

    a. Added THTR optional time to [   ]^{a,c} for control.

7.   **PUMP** See Section 10.4.

a. Added the [   ]^{a,c} as OPTION=3. Modifications in PUMPI, RDCRVS, RDDIM. See Figures 10-4 through 10-7 for the [
]^{a,c}.

b. Included the WC/T production version (WC/T Version Mod.7A Revision 7) [
]^{a,c}, with input of TFROPT=1 on input card PUMP.7.

8.   **TEE**   See Section 10.3.

a. Added [

]^{a,c}

applied in TF1D.

b. Added [

]^{a,c} applied

in PREPER.

c. Modified flow regime map (and use of inputs [   ]^{a,c}). Horizontal stratification in a TEE can be controlled by [
]^{a,c}. Calculations in FEMOM and HTIF. See Section 4.4.

d. Added new option under IOFFTK=1 to use [
]^{a,c}. See Section 6.3.6 for as-coded description and Section 17 for the assessment.

e. Modified [
]^{a,c}. Calculations in OFFTKE. See Section 5.13 for description of changes to the offtake model.

f. Added new IENTRN=4 option, with [   ]^{a,c}.

9.   **VALVE** See Section 10.7.

a. Added [

]^{a,c} applied in TF1D.

b. Added [

]^{a,c} applied in PREPER.

Question #48: Steam Generator Modeling

WCAP-16996-P/WCAP-16996-NP, Volumes I, II and III, Revision 0, Subsection 10.5, "Steam Generator," explains that PWR Steam Generator (SG) is modeled in WCOBRA/TRAC-TF2 with a combination of PIPE, TEE, and HTSTR components. The example noding diagram for a U-tube SG shown in Figure 10-8, "Steam Generator Noding Diagram," includes a single PIPE component representing the entire U-tube bundle. The SG models in the plant examples discussed in WCAP-16996-P/WCAP-16996-NP, Volumes I, II and III, Revision 0, Section 26, "WCOBRA/TRAC-TF2 Model of Pilot Plants," follow the same modeling approach. As seen from Figure 26.2-9, "Virgil C. Summer Steam Generator Component Noding Diagram," and Figure 26.3-15, "Beaver Valley Unit 1 Steam Generator Component Noding Diagram," the U-tube bundle is modeled with a single PIPE component as well.

Although WCAP-16996-P/WCAP-16996-NP, Volumes I, II and III, Revision 0, Subsection 10.5, "Steam Generator," mentions that in the implemented approach the SG U-tube bundle is represented by "a single effective tube that has the heat transfer characteristics of the entire tube bank," the following related items need further clarification.

Using a single PIPE in combination with a HTSTR component allows preserving the heat transfer surface area of the entire SG U-tube bundle. At the same time, individual U-tubes in the bundle are characterized by various elevation heights of the apex points in their bending sections that range between the height of the apex of the shortest tube raw and that of the longest tube raw. It is recognized that the height of individual U-tubes in the bundle is an important factor under conditions involving natural circulation through the primary coolant loops. Such conditions are of importance when modeling small break LOCAs. Accordingly, several U-tube rows of different heights are used in integral PWR test facilities to represent the SGs. For example, the PKL III (abbreviation from Primärkreislauf, German for primary coolant circuit) 1:1 vertical scale replica of a 1,300 MegaWatt PWR employs seven different U-tube clusters of variable height to represent the SG U-tube bundle. The elevation difference between the apex of the longest tube cluster and that of the shortest one amounts to 2.020 m or 6.63 ft (see Figure 2.3, "Axial Locations of Thermocouples in SG Tubes," in NUREG/IA-0170, "RELAP5/MOD3.2 Post Test Calculation of the PKL-Experiment PKLIII-B4.3", December 1999). As reported by K. Umminger, T. Mull, and B. Brand, "Integral Effect Tests in the PKL Facility with International Participation," Nuclear Engineering and Technology, Vol. 41, No. 6, pp. 765-774, August 2009, representing the SG tubes by three lengths can be insufficient for adequate modeling of processes in the SG tubes that are of importance for specific accident conditions.

Please explain and provide the technical basis in support of using a single PIPE representation of the SG U-tube bundle in WCOBRA/TRAC-TF2 models of plants with such SGs. Discuss possible limitations of this approach with regard to modeling thermal-hydraulic phenomena that can take place during small break LOCA transients using the FULL SPECTRUM™ LOCA methodology. Explain how it is ensured that the SG U-tube bundle representation and SG modeling are adequate in resolving specific processes of safety importance that can occur during the course of a small break LOCA.

Response:

<u>**Issue Description:**</u>

As noted in the RAI, the steam generator (SG) model used in the PWR plant examples in [1] uses a single PIPE component to model the entire primary side U-tube bundle; the primary-to-secondary heat transfer is modeled by using a HTSRT component connected inside to the U-tube PIPE and outside to the secondary side, modeled by the main pipe of a TEE component.

The particular concern of this RAI is that using a single PIPE component to model the steam generator U-tube bundle would not capture the effect of the possible flow stagnation or reversal in some of the U-tubes during the natural circulation (NC) phase of a small break loss of coolant accident (SBLOCA).

As stated in the RAI, results of some PKL mid-loop natural circulation tests investigating boron dilution have indicated the presence of unstable non-uniform SG U-tube behavior during the natural circulation phase of a mid-loop operation test. It is suggested in Section 4.3 of [2], based on benchmark simulation experience of PKL tests reported in [3], that more detailed multi-tube representation of the SG U-tubes is needed to capture the complex non-uniform multi-tube behavior during natural circulation. However, it has to be noted that this recommendation is made for the simulation of long-term boron dilution studies, not necessarily the early stages of LOCA accidents.

<u>**State of Knowledge (experimental and analytical):**</u>

Non-uniform U-tube flow behavior has been observed and reported by both the PKL boron dilution NC tests in [2] and [3] and the ROSA-IV LSTF natural circulation tests in [4],[5],[6], and [7].

As reported in Section 4.1 of [4], temperature measurements in the LSTF steam generator U-tubes during the high-pressure natural circulation test ST-NC-02 indicated that the flow in the longer U-tubes was stagnant or reversed in direction for mass inventories greater than 80%. More detailed discussion of the different flow modes observed in the LSTF U-tubes during the high-pressure NC test ST-NC-02 is presented in [5]. In particular, Fig.3 of [5] shows quite a complicated map of observed flow modes in the U-tubes at the different phases (system inventories) of natural circulation. For example, flow reversal is indicated to occur in the long and even some of the medium length U-tubes between 100% and 80% for system inventories. Cyclic fill&dump (F&D) is indicated to occur in all U-tubes for inventories between 80% and 62%, approximately. The process of emptying (E) occurs at inventories between 65% to 60%. Reflux condensation is established in all U-tubes for inventories less than 57% and in a typical SBLOCA would normally end when the loop seals clear.

As stated in [5], experience with modeling the LSTF natural circulation test ST-NC-02 with the RELAP5/MOD2 code using single-tube representation of the SG U-tube [6] suggested the need for more detailed multiple U-tube modeling for accurate prediction of the system overall response; the single-tube modeling approach resulted in over-prediction of the loop flow for single-phase NC and the loop flow oscillations were much larger than those observed in the test. However, the results of RELAP5/MOD3.3 simulations of the ST-NC-02 test with multiple SG U-tubes reported in [7] do not seem to have contributed much to the overall accuracy of the calculations. With a 9-tube

representation of the U-tubes, Fig.11 of [7], the average loop flow is still well over-predicted, for both single-phase and the two-phase period of the natural circulation. The effect of the 9-tube U-tube model is a significant reduction of the calculated loop flow oscillation, Fig.13 of [7], which can obviously be attributed to the 180-degree phase shift of the flows calculated in the 9 individual U-tubes, Fig.14 of [7], but not necessarily an ability to capture realistically the complex non-uniform U-tube flow modes observed in the test.

Calculations using the TRAC code and a 3-tube model of the U-tube SG bundle, reported in [8], appear to have resulted in only qualitative representation of the overall ST-NC-02 test results. However, although flow reversal was calculated to occur in the long U-tube during the single-phase NC period, and the peak flow was calculated to occur at the same system mass inventory as the test, the calculated overall maximum loop flow rate exceeded the measured by 50%. Uncertain and inconclusive explanation was offered in [8] to explain the discrepancies between the test and the simulation results.

In summary, it appears that the known attempts to explicitly model the non-uniform flow behavior in the SG U-tube bundle using a multi-tube representation do not add to substantial improvement of the accuracy in the calculated overall SG behavior during natural circulation.

Justification of the Single-PIPE Steam Generator U-tube Modeling Approach

The ROSA-IV Large Scale Test Facility (LSTF) is used as an important benchmark integral test facility to validate various component modeling techniques used by the PWR simulations within the Westinghouse FSLOCA Methodology [1], including that of the SG U-tube bundle model. Since the design and scaling of the ROSA-IV LSTF allows for the realistic reproduction of the most important small break thermo-hydraulic phenomena, the ROSA LSTF steam generator (SG) model was validated through the simulation of selected ROSA LSTF tests; consistent with the design similarity, the same SG modeling approach was adopted for the full scale PWR plant calculations as well, Section 26 of [1].

The significance and ranking of the steam generator multi-tube behavior during the different phases of the small, intermediate and large break LOCA is briefly discussed in Section 2.3.2.7 of [1].

Large and Intermediate Breaks:

As stated in Section 2.3.2.7 of [1], for intermediate and large breaks the multi-tube behavior has a low influence on the flow through the SG during all phases of the transient. A single-pipe representation of the SG U-tube bundle would be sufficiently to model the SG primary side behavior with respect to primary-to-secondary side heat transfer for intermediate and large break LOCA accidents.

Small Breaks, Blowdown Phase, (Single-Phase Natural Circulation):

With single-phase natural circulation complemented by the driving head of the reactor coolant pumps still coasting down, significant non-uniform U-tube behavior (flow stagnation and/or inversion observed in the PKL and the ROSA natural circulation tests) is unlikely to occur. Therefore, single-pipe modeling would be sufficient representation of the SG U-tube bundle thermal hydraulic behavior.

Small Breaks, Natural Circulation (Two-Phase):

For the purpose of the discussion herein, it is clarified that the "natural circulation (NC) period", as described in Section 2.3.1.1 of [1], in fact refers to the period of two-phase NC followed by the reflux condensation, which typically includes the loop seal clearing phenomenon; as mentioned above, the single-phase NC occurs earlier during the blowdown period.

The results of the simulation of the ROSA-IV LSTF high-pressure natural circulation test ST-NC-02, documented in Section 21.9 of [1] demonstrate that with the single-tube model of the SG U-tubes the calculated general system behavior is consistent with that observed in the test. Sufficient accuracy is achieved in calculating the loop flow rate at different primary side fluid inventories and phases of the natural circulation, Figure 21.9-2 of [1]. The calculated void fraction distribution as a function of system inventory (Figures 21.9-11 and 21.9-12 for SGA, and Figure 21.9-13 and 21.9-14 for SGB, [1]) indicate that the code is even capable of predicting in general the "cyclic fill & dump" phenomenon observed in the U-tubes at the ST-NC-02 test, as described in [5] and [7]. At the same time, as pointed out in Section 21.9.4, the calculated effective heat transfer coefficient is [   ]^{a,c} than the minimum measured at the LSTF post-natural circulation test ST-SG-02, reported in Section 4.2 of [4]. As a result, it is judged that with the current SG model (single-pipe U-tube) the code has the tendency to slightly [   ]^{a,c} the primary system pressure. As seen in Figure 21.9-3 (system inventories less than 80%), this effect appears to be relatively small, 0.25 MPa (36 psi), but is still in a conservative direction – [

                                                                                                    ]^{a,c}.

The calculations (Figure 21.9-4 for ST-NC-02 and Figures 21.4-7 and -8 for SB-CL-18, [1]) also indicate somewhat excessive liquid holdup in the uphill side of the steam generator U-tubes during the NC phase; this contributes to deeper and longer core uncovery and as a result higher rod heat-up during the loop seal clearance period.

In summary, it is concluded that the single-pipe modeling of the steam generator U-tubes represents reasonably well and in a conservative manner the most important thermo-hydraulic phenomena that might affect the key overall results (PCT, core coolability, etc.).

Small Break, Core Recovery and Boiloff:

During this phase of the SBLOCA accident the steam generator secondary side is a heat source, the tubes are essentially drained and vapor super-heating is the predominant phenomenon; non-uniform U-tube behavior is not expected to occur. Therefore, single-pipe U-tube bundle modeling is sufficient to model the secondary-to-primary side heat transfer.

Applicability and Limitations of the Single-PIPE SG Model:

It is obvious that the single-pipe representation of the SG U-tube model adopted for the FSLOCA methodology, as described in [1], is not capable to model localized non-uniform multi-tube behavior, in particular that related to boron dilution that might occur during long-term post-LOCA scenarios discussed in [2] and [3].

While the need to accurately represent the non-uniform U-tube behavior seems obvious for the purpose of boron dilution studies, that need is not as obvious for the class of LOCA transients considered within the Westinghouse FSLOCA methodology presented in [1], where the sequence of the NC phenomena developing during the accident are quite different. Therefore, based on the model validation, it is judged that the single-pipe SG U-tube model used for the PWR simulations represents conservatively and with sufficient detail key thermal hydraulic phenomena taking place in the SG during the different phases of the LOCA accidents considered by the Westinghouse FSLOCA Methodology [1], which exclude the long-term cooling period and associated boron dilution phenomena.

References:

1. WCAP-16996-P, "Realistic LOCA Evaluation Methodology Applied to the Full Spectrum of Break Sizes (FULL SPECTRUM™ LOCA Methodology)," November 2010.

2. Umminger, K., et.al., "Integral Effect Tests in the PKL Facility with International Participation," Nuclear Engineering and Technology, Vo.41, No.6, pp 765-774, August 2009.

3. A. Bucalossi, "Validation of Thermal-Hydraulic Codes for Boron Dilution Transients in the Context of the OECD/SETH Project", Seminar 2, EUROSAFE, Brussels, 2005.

4. Tasaka, K., et al., "The Results of 5% Small Break LOCA Tests and Natural Recirculation Tests at the ROSA-IV LSTF," Nuclear Engineering and Design, Vol.108, pp 37-44 (1988).

5. Y. Kukita, et.al., "Nonuniform Steam Generator U-Tube Flow Distribution During Natural Circulation Tests in ROSA-IV Large Scale Test Facility," Nuclear Science and Engineering: Vol. 99, pp 289-298 (1988).

6. JAERI-M 88-215, "Post-Test Analysis with RELAP5/MOD2 of ROSA-IV/LSTF Natural Circulation Test ST-NC-02," October 1988.

7. Yonomoto, T., "ROSA/LSTF Experiments of PWR Natural Circulation and Validation of RELAP5/MOD3.3," 2nd CRP RCM, Corvallis, Oregon (USA), Aug. 29–Sept. 2 (2005).

8. H. Stumpf, et.al., "Reverse Primary-Side Flow in Steam Generators During Natural Circulation Cooling," ASME Heat Transfer Division (HTD), Vol. 92. Submitted to ASME Winter Annual Meeting, Boston, Massachusetts, December 13-18 (1987).

Question #49: T-Junction Component

WCAP-16996-P/WCAP-16996-NP, Volumes I, II and III, Revision 0, Subsection 10.3, "TEE Component," explains that WCOBRA/TRAC-TF2 basically treats a TEE component as two PIPE components as shown in Figure 10-2, "TEE Component Noding." If the primary-side PIPE component, PIPE 1, has NCELL1 cells and the secondary-side PIPE component, PIPE 2, has NCELL2 cells, please explain the meaning of the parameter NCELLS, defined in Figure 10-2 by the expression NCELLS = NCELL1 + 1 + NCELL2.

Response:

The parameter NCELLS is defined by the expression NCELLS = NCELL1 + 1 + NCELL2, where NCELL1 is the number of cells in the main branch and NCELL2 is the number of cells in the side branch. There is one phantom cell in between the last index of the main branch and the first index of the side branch. The phantom cell represents [

]^{a,c} Users are not required to provide input related to the phantom cell, and the information of the phantom cell is not shown in the output file as well.

Question #50: Component Multipliers

WCAP-16996-P/WCAP-16996-NP, Volumes I, II and III, Revision 0, Section 10, "WCOBRA/TRAC-TF2 One-Dimensional Component Models," states that additional user-defined multipliers were added that enable the code user to affect specific models and correlations in WCOBRA/TRAC-TF2.

The HS_SLUG multiplier, identified in Subsection 10.2, "PIPE Component," can be used to affect the horizontal flow calculation for all WCOBRA/TRAC-TF2 one-dimensional hydraulic components, except the PUMP. According to Subsection 10.2, this multiplier ranges between 0.1 and 9.99. WCAP-16996-P/WCAP-16996-NP, Volumes I, II and III, Revision 0, Subsection 4.4.5, "Horizontal Stratified Flow," provides a range from 0.1 to 9.9 for the same parameter. Its default input value is equal to
[   ]^{a,c} and, according to WCAP-16996-P/WCAP-16996-NP, Volumes I, II and III, Revision 0, Subsection 17.3.4, "WCOBRA/TRAC-TF2 Results: Sensitivity Studies," its uncertainty range is from
[   ]^{a,c}

User specified allowances for horizontal stratification within a PIPE component can be provided through the MSTRTX and STRTX input. Similarly, the user has the option to specify allowance for horizontal stratification in the TEE main and side pipes through the STRTX1 and STRTX2 multipliers. The option to provide user specified allowance for horizontal flow is not available in the VALVE component model.

Interfacial drag multipliers YDRGX can be defined by the user at any cell faces of the PIPE, TEE and VALVE components. Similarly, interfacial condensation heat transfer at user selected cells can be modified by using the CNDNX multipliers for the PIPE and TEE components and the XCNDX multiplier for the VALVE component.

WCAP-16996-P Revision 0 Subsection 29.1.6, "Cold Leg Condensation (KCOSI)," identifies a cold leg condensation multiplier, KCOSI, that was added in the code to allow varying the cold leg condensation heat transfer rate for the purpose of the uncertainty analysis.

Please clarify the following items related to the use of user-defined multipliers in conjunction with the one-dimensional component models discussed in Section 10 of WCAP-16996-P/WCAP-16996-NP, Volumes I, II and III, Revision 0:

(1) Please provide a table that lists all user-defined multipliers that can be applied to the one-dimensional component models in WCOBRA/TRAC-TF2 presented in Section 10. For each multiplier, include its identifier, relevant one-dimensional component, applicable cells/interfaces, default value, and allowable range of input values as appropriate.

(2) Please identify the multipliers that are subject to sampling in the uncertainty analyses and provide a table that lists all such multipliers. For each such parameter, provide its identifier, sampling range and corresponding distribution. Explain the technical basis for establishing the provided sampling ranges and sampling distributions. Please explain each individual case for which the range of allowable input values for a multiplier is broader than the defined sampling range (e.g., HS_SLUG).

(3) For the multipliers that are not subject to sampling, if any, please explain the basis for introducing such multipliers. In addition, please clarify how the ranges of allowed input values were established and explain the process of determining the input values in performing plant analyses using the FULL SPECTRUM™ LOCA methodology. Explain if an input value in a plant model can fall outside of the documented range of allowable input values.

(4) Please address Items (1) through (3) above for user-defined multipliers that can be applied to VESSEL component models in WCOBRA/TRAC-TF2, as applicable.

Response:

Part (1)

Table 50-1 below provides a list of all user-defined multipliers that can be applied to the one-dimensional component models, as well as all user-defined multipliers that can be applied to VESSEL component models in WCOBRA/TRAC-TF2. [

]^{a,c}

Table 50-1: User Defined Multipliers

[					
					]^{a,c}

[

					]^{a,c}

---

[1] [   ]^{a,c}

[

]^{a,c}

[

$]^{a,c}$

Part (2)

Table 50-2 below specifies the multipliers from Table 50-1 that are subject to sampling in the uncertainty analysis. The first column in Table 50-2 specifies the multiplier name, and the second column provides a description of the multiplier. The third and fourth columns provide the sampling range and distribution of each multiplier, respectively. The final column in Table 50-2 (Reference) shows the section from WCAP-16996-P that explains the technical basis for establishing the provided sampling ranges and sampling distributions. If the applicable section from WCAP-16996-P does not provide a sufficient explanation, more detail is provided in the notes section of Table 50-2. It is noted that the basis for most of this information is the Westinghouse response to RAI 77.

Table 50-2: Multipliers Subject to Sampling in the Uncertainty Analysis

Acronym	Identifier	Sampling Range	Distribution	Reference
Multipliers Applicable to One-Dimensional Components				
[				
				]a,c

---

[1] [ ]a,c

[2] [ ]a,c

[3] [ ]a,c

[

				]^{a,c}

¹ [
                    ]^{a,c}
² [

                                        ]^{a,c}

[

$]^{a,c}$

Part (3)

Table 50-3 below lists the multipliers that are not subject to sampling in the uncertainty analysis. Additional information about each of these multipliers is in Table 50-1. In FSLOCA EM, the value for each of these multipliers is set at the default value, which is shown in both Table 50-1 and Table 50-3. The rationale for the default value which is fixed in the FSLOCA EM is provided in the 2nd column of Table 50-3. It is noted that there is a description for each of the multipliers that appears in Table 50-1 but does not appear in Table 50-2.

Table 50-3: Justification of Default Values for Multipliers Not Subject to Sampling in the Uncertainty Analysis

Identifier	Justification of the Default Value or the Value used in the FSLOCA EM

[

]^{a,c}

Identifier	Justification of the Default Value or the Value used in the FSLOCA EM

[

]^{a,c}

Question #51: Fluid Properties for Nusselt Number in Dispersed Droplet Flow

WCAP-16996-P/WCAP-16996-NP, Volumes I, II and III, Revision 0, Subsection 6.2.7, Dispersed Droplet Flow Regime," provides the interfacial heat transfer coefficient between superheated vapor and dispersed droplets in Equation (6-70), which can be presented in terms of the Nusselt number as follows:

[   ]^{a,c}

WCAP-16996-P/WCAP-16996-NP, Volumes I, II and III, Revision 0, Subsection 6.2.7 identifies [

]^{a,c}

Please clarify the following items related to the application of the above correlation for predicting the interfacial heat transfer from superheated steam to liquid droplets for dispersed droplet flow in WCOBRA/TRAC-TF2.

(1) Define the quantities used in Equation (6-71) to determine [
]^{a,c} Explain if B reduces to zero when the steam superheat becomes negligible. Explain how WCOBRA/TRAC-TF2 determines the thermodynamic properties that are used to calculate [
]^{a,c} in Equation (6-71).

(2) Under high-temperature superheated steam conditions, the Reynolds, Prandtl, and Nusselt numbers become significantly dependent on the fluid properties that are used to calculate the values. The values for these dimensionless numbers evaluated at the free stream (ambient) temperature can differ significantly from those evaluated at the film temperature. Usually, the temperature of the film formed around the droplet from vaporization is defined as the mean of the droplet surface temperature and the ambient gas temperature. Please explain which thermodynamic properties are used in WCOBRA/TRAC-TF2 to calculate the Reynolds, Prandtl, and Nusselt numbers in Equation (6-70).

Equation (6-70) is basically the [

]^{a,c}

Response:

WCT-TF2 calculates the interfacial heat transfer between the superheated steam and liquid droplets in the dispersed flow and film boiling (DFFB) flow regime using Equation (6-70) in Reference 1.

The mass transfer number, B, as shown in Equations (6-51) and (6-71) of Reference 1 involves typos and they should be corrected as follows:

[

$]^{a,c}$

With the correction as defined above, the mass transfer number, B, reduces to zero if no vapor phase superheating exists.

In Equation (6-70) of Reference 1, the Reynolds number Re_d and Prandtl number Pr_v are calculated

[

$]^{a,c}$

As function of flow Reynolds and Prandtl numbers without considering the correction to the vapor phase superheating, Equation (6-70) of Reference 1 is [
                     $]^{a,c}$. For example, the well-referenced Ranz and Marshall correlation (Reference

8) is presented in Equation RAI.5, among others recommended using different constants in front of the Reynolds number in the range of from 0.55 (Reference 2) to 0.74 (Reference 5).

$$Nu = 2.0 + 0.60 \, \mathrm{Re}_f^{1/2} \, \mathrm{Pr}_f^{1/3}$$ RAI.5

The Westinghouse topical report (Reference 1) refers Equation (6-70) therein as the [

]^{a,c} However,

Equation (6-70) of Reference 1 is different from the exact form of the [

]^{a,c} To assess the potential impact of using the [

]^{a,c} the WCT-TF2 DFFB interfacial heat transfer correlation, i.e. Equation (6-70) of Reference 1, is compared with the correlation recommended in Reference 5 in which the correlation is proposed for high temperature steam droplet flows, as shown in Figures RAI.1 and RAI.2 as follows. Please note that the Reference 5 correlation is recommended based on its comparison to the low pressure and high temperature air data available from Reference 3 and 4, which covers a pressure range lower than 30 psia and an air superheating range from 150 – 960 °C.

a,c

Figure RAI.1   Comparison of DFFB interfacial heat transfer correlations [   ]^{a,c}

a,c

Figure RAI.2   Comparison of DFFB interfacial heat transfer correlations [   ]^{a,c}

It is shown in the comparisons in these figures that WCT-TF2 predicts [

]^{a,c}. In most of the DFFB flows occur in WCT-TF2 plant simulations, their void fraction is in the range of [   ]^{a,c}. If the void fraction of [   ]^{a,c} is used in the comparisons shown in Figures RAI.1 and RAI.2 above, the WCT-TF2 [   ]^{a,c} would be less than [   ]^{a,c} relative to the Reference 5 correlation. The uncertainties introduced by the interfacial heat transfer models will be accounted for in WCT-TF2 as part of the [

]^{a,c} for DFFB heat transfer (Section 29.4.3 of Reference 1)

References:

1. WCAP-16996-P, "Realistic LOCA Evaluation Methodology Applied to the Full Spectrum of Break Sizes (FULL SPECTRUM^{TM} LOCA Methodology)," November 2010.

2. Forslund, R. P. and Rohsenow, W. M., "Dispersed Flow Film Boiling," J. Heat Transfer, Vol. 90, pp. 399-407, 1968.

3. Yuen, M. C. and Chen, L. W., "Heat-Transfer Measurements of Evaporating Liquid Droplets," Int. J. Heat Mass Transfer, Vol. 21, pp. 537-542, 1978.

4. Lee, K. and Ryley, D. J., "The Evaporation of Water Droplets in Superheated Steam," J. Heat Transfer, Vol. 90, pp. 445-451, 1968.

5. Ban, C. H. and Kim, Y., "Evaporation of a Water Droplet in High-Temperature Steam," J. Korean Nuclear Society, Vol. 32, pp. 521-529, 2000.

6. Ishii, M. and Chawla, T. C., "Local Drag Laws in Dispersed Two-Phase Flow," ANL-79-105, NUREG/CR-1230, 1979.

7. Wallis, G.B, "One Dimensional Two Phase Flow," McGraw Hill Book Company, 1969.

8. Crowe, C. T., Sommerfeld M. and Tsuji Y., "Multiphase Flows With Droplets and Particles,", CRC Press LLC, 1998.

Question #52: Nusselt Number Correlation Applicability for Dispersed Droplet Flow

WCAP-16996-P/WCAP-16996-NP, Volumes I, II and III, Revision 0, Subsection 6.2.5, "Inverted Annular Regime," explains that the coefficient [

]^{a,c} The same coefficient appears in Equation (6-70) in WCAP-16996-P/WCAP-16996-NP, Volumes I, II and III, Revision 0, Subsection 6.2.7, Dispersed Droplet Flow Regime," which provides the interfacial heat transfer coefficient between superheated vapor and dispersed droplets. Equation (6-70) can be presented as:

[   ]^{a,c}

As mass transfer away from the drop has been found to decrease the heat transfer, the effect of evaporation on the interfacial heat transfer needs to be accounted for if the free stream gas phase is superheated. The shielding function [   ]^{a,c} in Equation (6-70) accounts for steam superheating. Importantly, during the reflood phase of a PWR LOCA, the core seam flow conditions range from negligible to considerable steam superheating. For example, at a typical reflood pressure of 0.3 MPa and an assumed superheated steam temperature of 1,000 K (723 °C or 1,340 °F), the heat to increase the temperature of the evaporated steam to 1,000 K exceeds half of the latent heat of evaporation.

Yuen and Chen (1978) (M. C. Yuen and L. W. Chen, 1978, "Heat-Transfer Measurements of Evaporating Liquid Droplets," Int. J. Heat and Mass Transfer, Volume 21, Issue 5, pp. 537-542, May 1978) studied heat transfer to water and methanol droplets in an atmospheric vertical hot air tunnel and showed that the experimental data can best be correlated by:

$Nu_f = (2+0.6Re_M^{1/2} Pr_f^{1/3})/(1+B)$.

Their experiments were limited to the following range of flow conditions:

Reynolds number: 200 - 2,000
Pressure: atmospheric
Free stream air temperature: 150 - 960 °C (302 - 1,760 °F)
Velocity: 2.1 - 11.4 m/s (6.9 - 37.4 fps)

Renksizbulut and Yuen (1983) (M. Renksizbulut and M. C. Yuen, "Experimental Study of Droplet Evaporation in a High-Temperature Air Stream," J. Heat Transfer, Volume 105, Issue 2, pp. 384-388, May 1983) measured heat transfer rates to liquid droplets of water, methanol and heptane in an atmospheric hot air tunnel in a Reynolds number range of 25 to 2,000 and a Spalding number range of 0.07 to 2.79. It was shown that the obtained experimental data along with data by others can best be correlated by:

$Nu_f = (2+0.57Re_M^{1/2} Pr_f^{1/3})/(1+B)^{0.7}$.

Ban and Kim (2000) (Ch. Hw. Ban and Y. Kim, "Evaporation of a Water Droplet in High-Temperature Steam," J. Korean Nuclear Society, Volume 32, Number 5, pp. 521-529, October, 2000) proposed a modification to the Lee and Ryley (1968) correlation (K. Lee and D. J. Ryley, "The Evaporation of

Water Droplets in Superheated Steam," J. Heat Transfer, Volume 90, Issue 4, pp. 445-451, November 1968):

$$Nu_f = (2+0.74Re_M^{1/2} Pr_f^{1/3})/(1+B).$$

The proposed expression correlated well with data for a water droplet in gas flow for both negligible and considerable degree of superheating. Ban and Kim (2000) also explained that the necessity of the exponent 0.7 in the correlation by Renksizbulut and Yuen (1983) comes from the data of heptane and stated that water and methanol data can be well correlated with an exponent of 1.0. In this case, the correlation is identical with that by Yuen and Chen (1978) if radiation heat transfer is neglected in the calculation of the Spalding number as proposed by Renksizbulut and Yuen (1983).

A sensitivity study performed with the TRACE code by B. Belhouachi, S. P. Walker, and G. F. Hewitt, "Analysis and Computational Predictions of CHF Position and Post-CHF Heat Transfer," NUREG/IA-0236, May 2010, illustrated the central role of the droplet Nusselt number in the PCT and CHF predictions. Please clarify the following items related to the use of the correlation for predicting the interfacial heat transfer from superheated steam to liquid droplets for dispersed droplet flow in WCOBRA/TRAC-TF2.

(1) Identify the experimental data and provide the technical basis in support of the application of Equation (6-70) to calculate the interfacial heat transfer coefficient between superheated vapor and dispersed droplets in WCOBRA/TRAC-TF2. Describe the ranges of test conditions for which the applicable data sets were obtained and provide the applicability ranges for this equation.

(2) Present the technical basis for using a shielding function of [   ]^{a,c} in Equation (6-70). Applying different shielding functions to the same zero mass transfer Nusselt number can have a pronounced effect on the resulting heat transfer coefficient as the degree of superheating increases. For example, under typical reflood conditions at 0.3 MPa pressure and 1,000 K (1,340 °F) steam temperature, using a shielding function of [   ]^{a,c} with the same zero mass transfer Nusselt number will increase the predicted heat transfer coefficient by more than 20 percent Accordingly, this can have a pronounced impact on the calculated PCT.

(3) Demonstrate the applicability of Equation (6-70) for prediction of interfacial heat transfer between water droplets and superheated steam under the range of conditions occurring in a PWR core following a LBLOCA. Provide the expected ranges for the controlling flow parameters of interest for PWR LBLOCA re-flood analyses and compare these ranges against the test data conditions used to establish Equation (6-70) and its range of applicability. Discuss effects related to the correlation's applicability to PWR core flow re-flood conditions considering each governing parameter.

Response:

The heat transfer in DFFB is important for predicting fuel cladding temperatures during the blowdown and reflood phases of a large break LOCA and during the safety injection and accumulator injection phases of an intermediate break LOCA. WCT-TF2 calculates the total wall heat transfer by solving simultaneously the heat transfers from the wall to vapor, wall to liquid (continuous and entrained liquid) and between the vapor and liquid phases (Section 15.2, Reference 1).

In similar form as Equation (6-70) of Reference 1, several heat transfer correlations of evaporation of liquid droplets were recommended by a number of researchers (References 2, 3, 4 and 5) based on the experiments conducted using different fluids and under different thermal and flow conditions. None of the past experiments published were performed in sufficient high pressure and vapor temperature conditions using the water and superheated steam as those encountered in LOCA blowdown and reflood phases. For example, the tests reported in Reference 3 was performed using air at atmospheric pressure; Reference 2 conducted nitrogen film boiling convective heat transfer test under low pressure (inlet pressure was measured at 25 psia); the water/steam system was used in the test of Reference 4 with low degrees of vapor superheat (5~61 °F) and low pressure (14.7~28.9 psia); the effects of high degree of superheated air (150~960 °C) was investigated in the tests in Reference 3. Despite the limitation on these operating conditions, the tests cited above covered a comparable range of Reynolds number from 200 to 2000 with that during a typical large break LOCA low pressure reflood phase for DFFB flows.

The limits for the controlling parameters of DFFB interfacial heat transfer expected from PWR large break LOCA reflood phase are:[

$$]^{a,c}$$

The calculation of interfacial heat transfer is flow regime dependent in WCT-TF2 (Section 6.1, Reference 1). Equation (6-70) of Reference 1 is applied in predicting the interfacial heat transfer between the vapor and liquid droplet in DFFB flows occurring in high (blowdown, [$]^{a,c}$) and low (reflood, [$]^{a,c}$) pressure ranges. The DFFB interfacial heat transfer models in WCT-TF2 are validated in Sections 15.5 and 15.6 of Reference 1, through the comparison of the heater rod cladding temperatures with the available test data representative of the blowdown and reflood parameter ranges. Since fuel rod temperature is a direct indicator of the overall heat transfer between the rod and fluid, the interfacial heat transfer is thus validated as one of the contributors to the overall wall heat transfer, among the droplet size model, entrainment model, etc.

The DFFB heat transfer uncertainties (wall to vapor/droplet mixture) is accounted for through the DFFB heat transfer multipliers derived respectively for the blowdown and reflood phases in Section 29.4.3 of Reference 1. It is evident that the derived heat transfer multipliers include the bias introduced through the interfacial heat transfer model. In taking this approach to treat the overall uncertainties as a result of several contributing sub-models, it is realized that there exists potential compensating errors which could lead to a good match of the overall predicted results, e.g. cladding temperatures, to the test data, as a result of the lucky combination of the offsetting sub-model errors

under limited range of conditions. For example, under fixed flow conditions, the total wall heat transfer could be predicted reasonably well with over-predicted interfacial heat transfer coefficient, and under-predicted wall-vapor heat transfer coefficient. In interacting with hydraulic conditions, total wall heat transfer could also be reasonable due to a well predicted interfacial heat transfer as a result of the under-predicted interfacial heat transfer coefficient and over-predicted interfacial area (more entrainment or smaller droplet size).

The DFFB validation test data and WCT-TF2 prediction are analyzed in Section 24.6 of Reference 1, for potential compensating errors involved in the DFFB heat transfer during the large break blowdown and reflood phases. The intention there is to compare more available performance measures from the test with the code prediction than just the principle figures of merit, and demonstrate the physical and reasonable results in other areas than just the principle objectives. Specific to DFFB interfacial heat transfer, the pertaining discussion of compensating errors is summarized as follows for high (blowdown) and low (reflood) phases, respectively.

- High pressure (Blowdown, [   ]^{a,c})

  o DFFB validation using ORNL test data indicates that wall heat transfer is [

                    ]^{a,c} . Since most of the heat is transferred from the wall to the vapor phase which supplies the energy required for evaporating the liquid droplet in DFFB, [

                                                                                            ]^{a,c}.
     The total uncertainty of the wall heat transfer is accounted for by heat transfer multipliers as documented in Section 29.4.3 of Reference 1. There is no indication of compensating errors relating to the interfacial heat transfer in the total wall heat transfer from this validation.

  o G-1 Blowdown film boiling tests and WCT-TF2 simulation were compared and analyzed in Section 24.6.3. Based on the available test data, it was concluded that the observed [

                                                                                            ]^{a,c} .

- Low pressure (Reflood, [   ]^{a,c})

  o Section 24.6.4 of Reference 1 investigated DFFB heat transfer in one of the FLECHT SEASAT reflood tests and simulations. It was indicated that both the vapor superheat and cladding temperature above the quench front is [   ]^{a,c}, similar to several other forced reflood tests. Based on the comparison of vapor mass flow, droplet velocity, heat transfer to vapor and liquid phases above the quench front, the analysis therein shown that [

                                            ]^{a,c} .

The mass transfer from the liquid droplet during the evaporation has been found to decrease the heat transfer. To account for the effects of the mass transfer on the heat transfer process, the mass transfer number B is included in Equations (6-56), (6-57) and (6-70) of Reference 1 to extend their applicability in the case of high evaporation rate caused by superheated vapor. The form of the correction factor to the vapor phase superheating in Equation (6-70) of Reference 1, [

]^{a,c}. Yuen and Chen (Reference 3) and Ban and Kim (Reference 5) used a factor of 1.0/(1.0+B) to fit the experimental data in an attempt to account for the effect of vapor superheating on a heat transfer model assuming negligible mass transfer. However, no theoretical basis is provided in terms of using the form of 1.0/(1.0+B) to fit the test data, which validated the overall interfacial heat transfer models instead of just the correction factor of the vapor superheating.

It is true that under typical reflood conditions at 0.3 MPa pressure and 1,000 K (1,340 °F) steam temperature, using a shielding function of [   ]^{a,c} instead of 1/(1+B) with the same zero mass transfer Nusselt number will increase the predicted heat transfer coefficient by more than 20%. However, for most of the applied range in the large break LOCA reflood phase, as shown in the comparison figures, Figure RAI.1 and RAI.2, in the response to RAI #51, [

]^{a,c}.

The comparison difference shown therein is due to [

]^{a,c}.

References:

1. WCAP-16996-P, "Realistic LOCA Evaluation Methodology Applied to the Full Spectrum of Break Sizes (FULL SPECTRUM™ LOCA Methodology)," November 2010.

2. Forslund, R. P. and Rohsenow, W. M., "Dispersed Flow Film Boiling", J. Heat Transfer, Vol. 87, pp. 399-407, 1968.

3. Yuen, M. C. and Chen, L. W., "Heat-Transfer Measurements of Evaporating Liquid Droplets," Int. J. Heat Mass Transfer, Vol. 21, pp. 537-542, 1978.

4. Lee, K. and Ryley, D. J., "The Evaporation of Water Droplets in Superheated Steam," J. Heat Transfer, Vol. 90, pp. 445-451, 1968.

5. Ban, C. H. and Kim, Y., "Evaporation of a Water Droplet in High-Temperature Steam," J. Korean Nuclear Society, Vol. 32, pp. 521-529, 2000.

6. Wallis, G.B, "One Dimensional Two Phase Flow," McGraw Hill Book Company, 1969.

Question #53:   Interfacial Heat Transfer in Inverted Annular and Liquid Slug Flows

WCAP-16996-P/WCAP-16996-NP, Volumes I, II and III, Revision 0, Subsection 6.2.5, "Inverted Annular Regime," provides expressions for calculation of the interfacial heat transfer coefficient from both continuous liquid and droplets to superheated vapor for inverted annular flow in Equations (6-56) and (6-57). Subsection 6.2.6, "Inverted Liquid Slug Regime," defines the correlations for prediction of the interfacial heat transfer coefficient from the continuous liquid and droplets interface to superheated vapor for inverted liquid slug flow in Equations (6-65) and (6-66). The interfacial heat transfer coefficients given by the above identified equations can be presented in terms of the Nsselt number with a single expression:

[$]^{a,c}$

Please clarify the following items related to the use of the above correlation for predicting the interfacial heat transfer coefficient for inverted annular and inverted liquid slug flows in WCOBRA/TRAC-TF2.

(1) Describe the way of determining the fluid properties in calculating the Reynolds, Prandtl, [
        $]^{a,c}$ and Nusselt numbers in Equations (6-56), (6-57), (6-65), and (6-66) as applied in WCOBRA/TRAC-TF2 in the case of inverted annular and inverted liquid slug flows.

(2) Please present the technical bases and justify the applicability of Equations (6-56), (6-57), (6-65), and (6-66) for computing the interfacial heat transfer coefficient for inverted annular and inverted liquid slug flows in WCOBRA/TRAC-TF2.

Response:

WC/T-TF2 calculates the flow regime dependent interfacial heat transfer between the superheated vapor and the continuous liquid column and entrained droplets in the inverted annular and inverted liquid slug flow regimes using the Equations (6-56), (6-57), (6-65), (6-66) in Reference 1. In terms of flow regime, [

                                                                $]^{a,c}$. In these two regimes, referred to as hot wall regimes, the continuous liquid is assumed to be liquid column or slug separated from the hot wall by a thin vapor film, into which liquid droplet could be entrained.

WC/T-TF2 total wall heat transfer is determined by the overall interactions of the wall to vapor, wall to liquid and vapor to liquid phases. The total heat transfer from the wall to the fluid determines the fuel rod cooling/heating, which is the ultimate concern of LOCA transient simulation. Under those flow regimes, the wall heat transfer modes is selected based on the cell void fraction. More specifically, the inverted annular film boiling (IAFB) and dispersed flow film boiling (DFFB) modes feature low void fraction [$]^{a,c}$ and high void fraction [$]^{a,c}$, respectively. The interfacial heat transfer associated with the DFFB heat transfer mode is discussed in the Westinghouse Response to RAI 52. When [$]^{a,c}$, the wall heat transfer calculation is a simple interpolation between the IAFB and DFFB models.

The discussion in this response complements the Response to RAI 52 for DFFB mode with the interfacial heat transfer for the inverted annular/liquid slug flow regimes.

(1)   Equations (6-57) and (6-66) are used to calculate interfacial heat transfer from the superheated vapor to the entrained liquid droplets in the vapor phase. The fluid properties involved in these correlations are assessed [

   ]^{a,c}.

The interfacial heat transfer between the superheated vapor and the continuous liquid column is evaluated using Equations (6-56) and (6-65), which are [,

   ]^{a,c}. Details in evaluating the fluid properties involved in Equations (6-56) and (6-65) are presented as below:

[

   ]^{a,c}.

The impact of using [

   ]^{a,c} in the interfacial heat transfer models was evaluated in the Westinghouse response to RAI 51 for dispersed droplet flow regime. It was shown that WCT-TF2 [
   ]^{a,c} the interfacial heat transfer at extreme vapor superheat and high vapor Reynolds number. [

   ]^{a,c}

(2)   For interfacial heat transfer between the superheated vapor and liquid droplets, similar correlations as Equations (6-57) and (6-66) were developed by several researchers based on the experiments using different fluids, and more discussion of their models were presented in the Westinghouse Response to RAI 51 with respect to the interfacial heat transfer in the dispersed droplet flow regime.

In inverted annular and inverted liquid slug regimes, the continuous liquid column is assumed to be in the form of large liquid slugs, and [

]^{a,c} are utilized to calculate the interfacial heat transfer between the vapor and liquid column, assuming [

]^{a,c}. Reference 2 validated the application of Equation RAI.3 in air and water experiment with large droplets of up to 1.5 inches in diameter, which demonstrated that [

]^{a,c}.

$$Nu = 2.0 + 0.69 \, \text{Re}_v^{1/2} \, \text{Pr}_v^{1/3} \qquad\qquad \text{RAI.3}$$

In WC/T-TF2's applications to PWR plant simulation, the [

]^{a,c}.

The WC/T-TF2 interfacial heat transfer correlations (Equations (6-56), (6-57), (6-65), (6-66) in Reference 1) for the inverted annular and inverted liquid slug flow regimes are validated as [

]^{a,c}.

As explained in the WC/T-TF2 wall heat transfer models for the inverted annular film boiling in Section 7.2.6 of Reference 1, the total heat transfer from the wall is calculated using the [

]^{a,c}.

a,c

[

]^{a,c}

[

]^{a,c}.

For WC/T-TF2 applications, the inverted annular and inverted liquid slug regimes are [

]^{a,c}. Section 15.6.1.1.5 of Reference 1 documents the high flooding rate (6.1 in/s) validation test FLECHT SEASET Test 31701, and it is shown that WC/T-TF2 predicts [

]^{a,c}.

References:

1. WCAP-16996-P, "Realistic LOCA Evaluation Methodology Applied to the Full Spectrum of Break Sizes (FULL SPECTRUM™ LOCA Methodology)," November 2010.

2. Rowe, P. N., Claxton K. T. and Lewis, J. B., "Heat and Mass Transfer from A Single Sphere in An Extensive Flowing Fluid," Trans. Inst. Chem. Engrs., Vol. 43, 1965.

Question #54: Interfacial Heat Transfer to Droplet/Bubble

WCAP-16996-P/WCAP-16996-NP, Volumes I, II and III, Revision 0, Subsection 6.2.3, "Churn-Turbulent Regime," provides an expression for the interfacial heat transfer coefficient from superheated vapor to liquid droplets that can appear in the flow from entrainment and from adjoining channels. It states that "the interfacial heat transfer coefficient is given by the Lee-Ryley (1968) correlation," which is given in Equation (6-26). The relationship can be presented in terms of the Nusselt number as:

$$Nu_d = 2 + 0.74 Re_d^{1/2} Pr_v^{1/3}.$$

The correlation by K. Lee and D. J. Ryley, "The Evaporation of Water Droplets in Superheated Steam," J. Heat Transfer, Volume 90, Issue 4, pp. 445-451, November 1968, is given a special recognition in LOCA analyses as it was based on data for droplet evaporation in superheated steam in contrast to other experiments that studied liquid droplet evaporation in air. The droplet diameter and flow parameters were varied as follows:

Droplet diameter: 230 µm - 1,130 µm (9 mils - 44.5 mils)
Reynolds number: 64 - 250
Pressure: 101.4 - 200 kPa (14.7 - 29 psia)
Superheat: 2.8 - 33.9 K (5 - 61 °F)
Velocity: 2.7 - 11.9 m/s (9 - 39 fps)

WCAP-16996-P/WCAP-16996-NP, Volumes I, II and III, Revision 0, Subsection 6.2.7, "Dispersed Droplet Flow Regime," refers to [

]^{a,c}

[   ]^{a,c}

WCAP-16996-P/WCAP-16996-NP, Volumes I, II and III, Revision 0, Subsection 6.2.2, "Small to Large Bubble Regime," explains that the heat transfer coefficient for large bubbles of superheated vapor for the discussed flow regime is determined using the correlation by Lee and Ryley (1968) as given in Equation (6-14).

Please clarify the following items related to the prediction of the interfacial heat transfer from superheated steam to liquid droplets and from large superheated bubbles to the continuous liquid phase for different flow regimes in WCOBRA/TRAC-TF2.

(1) Explain why two different existing correlations are provided in WCAP-16996-P/WCAP-16996-NP, Volumes I, II and III, Revision 0, Section 6, "WCOBRA/TRAC-TF2 Interfacial Heat and Mass Transfer Models," when describing the technical basis for predicting interfacial heat transfer from superheated steam to liquid droplets.

(2) Equation (6-49) with small variations in the coefficient of the second term (0.552, 0.55, 0.60) is often cited in the technical literature. In the case of a liquid droplet falling through a moving airstream, Frössling (1938) developed an empirical relation of the same form for the mass transfer

number (Frössling, "Über die Verdunstung fallender Tropfen," Gerlands Beitrage Zur Geophysik, Volume 52, pp. 170-216, 1938). Ranz and Marshall (1952) used the heat transfer analogy to show that the heat transfer data can be correlated through the droplet Nusselt number using a relationship of the same form (see W. E. Ranz and W. R. Marshall, Jr.: "Evaporation from Drops: I," Journal of Chemical Engineering Progress, Volume 48, No. 3, pp. 141-146, March 1952. Also W. E. Ranz and W. R. Marshall, Jr.: "Evaporation from Drops: II," Journal of Chemical Engineering Progress, Volume 48, No. 4, pp. 173-180, April 1952). Please provide the reasons for its identification as "a correlation by Forslund and Rohsenow (1968)."

(3) According to Abou Al-Sood (2010), the Frössling (1938) and Ranz and Marshall (1952) correlations are applicable to describe droplet evaporation in a laminar convective flow (see M. M. Abou Al-Sood, "Simple Model for Turbulence Effects on the Vaporization of Liquid Single Droplets in Forced Convective Conditions," 23rd Annual Conference on Liquid Atomization and Spray Systems, ILASS – Europe 2010, Brno, Czech Republic, September 2010). Please explain the applicability of the Lee-Ryley (1968) correlation under flow conditions expected in a PWR core following a LBLOCA.

(4) The Lee and Ryley (1968) correlation was developed from data describing heat transfer from evaporating droplets. Although Subsection 6.2.2, "Small to Large Bubble Regime," recognizes that such bubbles are unlikely to occur extensively in a LOCA transient, please justify the technical basis for the use of the Lee and Ryley (1968) correlation for the description of heat transfer mechanisms in the case of large bubbles of superheated steam.

Response:

The RAI has four components. Part (1) of the questions asks to describe the technical basis for the different coefficient applied to the droplet Reynolds number Re_d in the calculation of the Nusselt number Nu_d. In particular a coefficient of [

$]^{a,c}$.

The first observation is that, as discussed in Section 6.2.3 of the TR, the Churn-Turbulent Regime is [

$]^{a,c}$.

Considering that a) [$]^{a,c}$ and b) [

$]^{a,c}$ to the

overall heat transfer from the vapor to the liquid.

On the contrary the Dispersed Droplet Flow Regime is one of the important hot wall flow regimes which are relevant to determine the heat transfer in proximity of the PCT location. In that regime the continuous liquid flow becomes completely entrained and the interfacial heat transfer is limited to the heat transfer between the superheated vapor and the droplets. Moreover, in the regime a high degree of superheating is anticipated.

As result, rather than addressing [

]^{a,c}, the focus in this response is to address the adequacy of the formulation used for the Dispersed Droplet Flow Regime which is the topic of parts (2) and (3) of this RAI.

Part (2) of the question acknowledges that [

]^{a,c}. Frossling (1938) (Reference 1) assumes 0.55, Ranz and Marshall (Reference 2) is based on 0.6 for example. [

]^{a,c}.

In part (3) the reviewer noted that Frossling-type of correlations, like Ranz-Marshall (Reference 2) and Lee-Ryley (Reference 4) correlations are applicable to droplet evaporation in a laminar convective flow. A review of the effect of turbulence on the combustion spray system evaporation rate of droplets is presented by Birouk (Reference 5) and a model is proposed in the cited reference of Abou Al-Sood (Reference 6) by the reviewers. In general, the review found that the turbulence acts as an enhancer to the interfacial heat and mass transfer, depending on the mean flow characteristics and the level of the turbulent intensity, among other spray droplet properties and spray environment conditions. Moreover, based on the review, the developed models to account for the turbulence effects on the interfacial heat and mass transfers requires the knowledge of the turbulent flow parameters, for example turbulent intensity, turbulent length scale, etc., [

]^{a,c}.

Section 24 further investigates the possibility of compensating errors which would originate by a bias on interfacial heat transfer in the DFFB regime. Section 24.6.3 discusses the observed [

]^{a,c}. However [

]^{a,c}.

Section 24.6.4 elaborates on the role of the interfacial heat transfer during reflood, by [

]^{a,c}.

Overall the potential for compensating error is understood and controlled and [

]^{a,c}.

Finally point (4) of the question asks to justify the use of the [

•

]^{a,c}.

Given the context in which it is used, the [   ]^{a,c} is a reasonable [

]^{a,c}.

References

1. Frossling, N., On the Evaporation of Falling Droplets. Gerlands Beitrage zur Geophysik, Vol. 52, 1938, pp. 170–216 (in German).

2. Ranz, W. E. and Marshall, W. R.,: Evaporation from Drops, Pt. 1. Chem. Eng. Prog., Vol. 48, 1952, pp. 141-146.

3. Forslund, R. P., and Rohsenow, W. M., "Dispersed Flow Film Boiling," J. Heat Transfer, Vol. 87, 1968, pp. 399-407.

4. Lee, K., and Ryley, D. J., "The Evaporation of Water Droplets in Superheated Steam," Trans A.S.M.E. J Heat Transfer, Vol. 90, 1968, pp. 445-451.

5. Birouk, M., and Gökalp, I., "Current status of droplet evaporation in turbulent flows," Progress in Energy and Combustion Science, Vol. 32, 2006, pp. 408–423

6. M. M. Abou Al-Sood, "Simple Model for Turbulence Effects on the Vaporization of Liquid Single Droplets in Forced Convective Conditions," ILASS – Europe 2010, 23rd Annual Conference on Liquid Atomization and Spray Systems, Brno, Czech Republic, September 2010

Question #55: Droplet Diameter for Interfacial Heat Transfer in Dispersed Droplet Flow

The liquid droplet diameter is an important parameter when computing the interfacial heat transfer for dispersed droplet flow. Considering single isolated droplet, the heat transfer coefficient decreases with increasing droplet diameter. However, the product of the heat transfer coefficient and the surface area will increase by virtue of surface area's higher order dependence on diameter. For a dispersed droplet flow at a certain flow quality, the product of the heat transfer coefficient and the integral droplet surface area will decrease when increasing the assumed droplet diameter as both the heat transfer coefficient and the integral surface area of all droplets will decrease.

WCAP-16996-P/WCAP-16996-NP, Volumes I, II and III, Revision 0, Subsection 6.2.7, "Dispersed Droplet Flow Regime," does not explain how the droplet size is determined for the purpose of predicting the interfacial heat transfer coefficient and associated heat transfer rate between the dispersed droplets and the continuous gas phase.

Please explain and justify the implemented modeling approach for calculating the droplet size in predicting the interfacial heat transfer between superheated steam and liquid droplets in addition to the information provided in Subsection 6.2.7, "Dispersed Droplet Flow Regime."

Response:

The dispersed droplet flow regime is one of the vessel hot wall flow regimes, characterized with the presence of a heated surface with a temperature exceeding that given by Equation 4-1. The heat transfer rate of the dispersed droplet is a product of the droplet heat transfer coefficient and the integral droplet surface area as shown by Eqs. 6-75 through 6-78 in Section 6.2.7. Both the heat transfer coefficient and droplet surface area depend on the droplet diameter. The dependence of the heat transfer coefficients on the droplet diameter is shown in both the Nusselt number and the Reynolds number. The interfacial area of droplets phase is explicitly tracked by the 3D module of W̲COBRA/TRAC-TF2. Thus, the droplet transportation mechanism, droplet generation mechanisms, evaporation/condensation, and droplet break up mechanism all contribute to the droplets interfacial area distribution and in turn determines the droplet diameter in the droplet heat transfer calculation. In the response, the interfacial area transport model and heat transfer coefficient in the dispersed droplet flow regime are explained in details.

The calculation of the interfacial area of the droplet field in the dispersed droplet flow regime is provided in Section 4.3.4. The interfacial area concentration (interfacial area in a unit volume) is determined directly from solution of the droplets interfacial area transport equation as shown in Section 4.3.7. Eq. 4-68 of Section 4.3.7 describes that the rate change of interfacial area concentration is a result of the convection of the interfacial area concentration, interfacial area concentration generated by entrainment and de-entrainment and the interfacial area concentration change due to phase change. The spacer grid droplet break up model in Section 5.6.5 also contributes to the interfacial area concentration. The discretized form of Eq. 4-68 is given in Eq. 4-76. The total droplet interfacial area is the interfacial area concentration times the volume of node as shown in Eq. 4-78. In general, the droplet interfacial area concentration is inversely proportional to the droplet diameter with a given droplet volume. The droplet interfacial area transport model is based on

sound transport theory and mechanistically captures the evolution of the interfacial area of the dispersed droplet fields.

The interfacial heat transfer coefficient models for the dispersed droplet flow regime are described in Section 6.2.7. The interfacial heat transfer between the superheated steam and liquid droplets is a result of heat transfer to the superheated vapor and heat transfer to subcooled liquid droplet. The interfacial heat transfer coefficient to superheated vapor is given by the modified Forslund-Rohsenow correlation (Eq. 6-70), where the droplet diameter appears as a part of Nusselt number and the heat transfer coefficient shows a low order dependence on the Reynolds number. Further discussion on modifying Forslund-Rohsenow correlation has been provided in Section 6.2.5. The interfacial heat transfer coefficient to subcooled liquid droplets is calculated using Andersen's formula (Eq. 6-73), where the droplet diameter only appears as a part of the Nusselt number. In those heat transfer models, the drop diameter of the dispersed droplet flow regime is calculated from the droplet volumetric fraction and interfacial area concentration as shown by Eq. 4-48 in Section 4.2.5. The calculated droplet diameter is limited to [

]^{a,c}

In addition, the FSLOCA topical report provides an assessment on the droplet model in the 3-D vessel module of WCOBRA/TRAC-TF2 in Section 15.9.2, where the predicted droplet size is compared with the measured droplet size from [

]^{a,c}

Question #56: Droplet-Wall Direct Contact Heat Transfer in Dispersed Flow Film Boiling

WCAP-16996-P/WCAP-16996-NP, Volumes I, II, and III, Revision 0, Subsection 7.2.7, "Dispersed Flow Film Boiling," explains that the VESSEL component wall heat transfer logic in WCOBRA/TRAC-TF2 invokes the Dispersed Flow Film Boiling (DFFB) heat transfer regime when the void fraction is greater than [$]^{a,c}$ and the wall temperature is greater than the minimum stable film boiling temperature, T_{MIN} as given in Equation (7-91). The subsection states that heat transfer in this post-dryout or post-CHF flow regime "is calculated as a "two-step" method where the dominant heat transfer mode is forced convection to superheated steam." The code computes the dispersed flow film boiling heat flux as a sum of four components: (1) convective heat flux to vapor, (2) radiative heat flux to vapor, (3) radiative heat flux to droplets, and (4) drop-wall direct contact heat transfer. What is also important, Subsection 7.2.7 explains that "the steam superheat is then determined by the interfacial heat transfer rate to the entrained droplets as part of the hydrodynamic solution."

Subsection 7.2.7 states that the drop-wall direct contact heat transfer that accounts for droplet impingement on the heated surface is calculated using the model by R. P. Forslund and W. M. Rohsenow, "Dispersed Flow Film Boiling," J. Heat Transfer, Vol. 90, Issue 4, pp. 399-407, November 1968, as given in Equation (7-130).

WCOBRA/TRAC-TF2 implements [

$]^{a,c}$

Following the initial surge into the core, the PWR core re-flood after a LBLOCA takes place at low flow and low pressure conditions. Flooding rates are very low and typically stay below 1 in/s. Under such conditions, post-dryout heat transfer with dispersed flow film boiling in the upper core region controls the PCT. For example, a typical re-flood flow rate of 0.8 in/s (0.02 m/s) of safety injection water at 150 °F (65.6 °C of 338.7 K) and 20 psia (1.4 bar or 0.14 MPa) corresponds to a mass flux of:

ρw (338.7 K, 0.14 MPa) x $V_{Reflood}$ = 980.3 kg/m³ x 0.02 m/s = 19.9 kg/m²-s = 14,687 lbm/ft²-hr.

For a fuel rod with a standard diameter of 0.422 inches (10.7x10⁻³ m) and an assumed peak LHGR of 15 kW/ft (49.2 kW/m), the linear heat rate and rod surface heat flux conditions for decay heat power ratios of 5 percent, 3 percent, and 2 percent (about 10 sec, 100 sec, and 1,000 sec after scram) are given in the Table 1 below.

Table 1: Fuel Rod LHGR and Surface Heat Flux Conditions

Parameter	Units	Value			
Decay Ratio	-	1.0	0.05	0.03	0.02
Decay Time	s	0.0	~10	~100	~1,000
LHGR	kW/ft	15	0.75	0.45	0.30

	kW/m	49.2	2.46	1.48	0.98
Heat Flux	Btu/(ft²-hr)	463,298	23,165	13,899	9,266
	kW/m²	1,461	73.1	43.8	29.2

Typical dispersed flow film boiling conditions at low reflood rate can be identified as:

Pressure: 1 to ~3 bar (0.1 to ~0.3 MPa or 14.5 to ~44 psia),

Mass Rate: ~1 in/s (0.0254 m/s) or ~25 kg/m²-s (18,700 lbm/ft²-hr),

Void Fraction: Higher than 80 percent.

A work by M. Andreani and G. Yadigaroglu, "Prediction Methods for Dispersed Flow Film Boiling," Int. J. of Multiphase Flow," Vol. 20, p. 1-51, 1994, and more recently a report by the International Atomic Energy Agency (IAEA), "Thermohydraulic Relationships for Advanced Water Cooled Reactors," IAEA-TECDOC-1203, April 2001, represent a comprehensive review of post-dryout heat transfer methods for water cooled reactors. NUREG/CR-6975, "Rod Bundle Heat Transfer Test Facility Test Plan and Design," July 2010, summarizes the available single-tube and rod bundle data and existing modeling approaches.

As discussed by M. Andreani and G. Yadigaroglu, "Difficulties in Modeling Dispersed-Flow Film Boiling," Wärme und Stoffübertragung, Volume 27, Number 1, pp. 37-49, 1992, the difficulties in the post-dryout heat transfer modeling are related to phenomenological characteristics of participating processes can be grouped into four major areas: (1) thermal non-equilibrium effects, (2) mechanical non-equilibrium effects, (3) flow history dependant heat transfer, and (4) sub-channel and spacer grid effects in fuel rod bundles. In addition, a major limitation is related to the area averaging aspect of any one-dimensional (1D) modeling approach that is used in LOCA analyses.

Thermal non-equilibrium effects are related to significant steam superheats have been measured in reflood experiments performed both with single-tube and rod bundle test sections. For example, Ghazanfari, A., Hicken, E. F., and Ziegler, A., "Unsteady Dispersed Flow Heat Transfer Under Loss-of-Coolant Accident Related Conditions," Nuclear Technology, Vol. 51, pp. 21-26, November 1980, measured vapor superheat of 260 K (468 °F) on average at the top of the test tube. More recent experiments by S.-Ki Moon et al., "An Experimental Study on Post-CHF Heat Transfer for Low Flow of Water in a 3x3 Rod Bundle," Nuclear Engineering and Technology, Vol. 37, No. 5, October 2005, also showed a significant degree of thermal non-equilibrium near the end of the heated length of a 3x3 test section. Mechanical non-equilibrium effects are related to the behavior of clusters of droplets in the continuous steam flow. M. Andreani and G. Yadigaroglu, "Effect of the Cross-Sectional Droplet Distribution in Dispersed Flow Film Boiling at Low Mass Flux," Proceedings of the 5th International Topical Meeting on Reactor Thermal-Hydraulics (NURETH-5), Volume III, pp. 823-831, September 21-24, 1992, Salt Lake City, Utah, USA, discuss related effects on prediction results obtained with 1D models. A recent work by F. B. Cheung and S. M. Bajorek, "Dynamics of Droplet Breakup Through a Grid Spacer in a Rod Bundle," Nuclear Engineering and Design, Vol. 241, pp. 236-244, 2011, focused on the dynamics of droplet breakup associated with the flow of a dispersed two-phase mixture through a rod bundle grid spacer during a PWR re-flood transient and presented new test data from the RBHT Facility.

Andreani and Yadigaroglu (1992) pointed out to modeling limitations related to the assumption of a uniform droplet distribution over the channel cross section. Importantly it was recognized that 1D models can overestimate the interfacial heat transfer between vapor and droplets if a cross-section averaged temperature difference between vapor and droplets is used instead of a temperature difference based on a lower mean temperature of vapor in the central core region where droplets tend to reside. As a result, such models can fail to adequately predict the wall surface temperature particularly at low flow conditions of interest for DFFB modeling.

Please clarify the following items related to the method of calculating the dispersed flow film boiling heat flux in WCOBRA/TRAC-TF2.

1. Explain what corrections and modeling features are applied in WCOBRA/TRAC-TF2 to overcome the major difficulties in modeling the dispersed flow film boiling with regard to both the interfacial and wall to fluid heat transfer processes. In addition, please explain how the limitation of the 1D approach stemming from the highly non-uniform steam temperature profile across the radial flow direction (maximum steam temperature near the wall with a cooler core region containing droplets) is rectified.

2. The Forlsund-Rohsenow (1968) correlation is based on data for dispersed flow film boiling of nitrogen under the following conditions:

Mass flux:	70,000 to 190,000 lbm/ft^2-hr (94.9 kg/m^2-s to 257.7 kg/m^2-s)
Heat flux:	5,000 to 25,000 Btu/ft^2-hr (15.8 to 78.9 kW/m^2)
Test section inlet pressure:	25 psia (1.72 bar or 0.172 MPa)
Test section exit quality:	35 percent to 315 percent
Test section inner diameter:	0.228 in, 0.323 in, 0.462 in (5.79 mm, 8.20 mm, 11.73 mm)

   Please present a table that includes typical ranges for conditions incurring during reflood dispersed flow film boiling in a PWR core and compare those against the Forlsund-Rohsenow (1968) test data conditions. Present comparison against data that representative of prototypical reflood conditions to support the WCOBRA/TRAC-TF2 dispersed flow film boiling model for prediction of PWR reflood PCTs.

   Heat transfer from a heated tube to dispersed steam-water flow under post-dryout conditions was studied experimentally by Ghazanfari, A., Hicken, E., and Ziegler, A., "Unsteady Dispersed Flow Heat Transfer Under Loss-of-Coolant Accident Related Conditions," Nuclear Technology, Vol. 51, pp. 21-26, November 1980. The test conditions varied as follows:

Mass flux:	10,300 to 26,500 lbm/ft^2-hr (14 to 36 kg/m^2-s)
Heat flux:	5,400 to 13,300 Btu/ft^2-hr (17 to 42 kW/m^2)
Pressure:	17.4 to 23.2 psia (1.2 to 1.6 bar)
Inlet quality:	0.50 to 1.00

As already mentioned, vapor superheat of 260 K (468 °F) on average was measured at the top of the test tube in the tests. It was also concluded that the wall droplet contribution to the total heat transfer rate was negligible at flow qualities greater than 50 percent.

The Forlsund-Rohsenow (1968) correlation is based on an equilibrium model where the bulk vapor temperature is assumed to be equal to the local saturation temperature. As such, its validity as a model basis for predicting direct contact heat transfer for the dispersed droplet field in WCOBRA/TRAC-TF2 is questionable. In addition, the use of this correlation above the quench front where the clad temperature is above the minimum stable film boiling temperature, T_{MIN}, and significant steam superheating can take place is considered inappropriate. Once the liquid droplets enter into the central flow region, there can be insufficient lateral momentum that is needed for them to penetrate the highly superheated boundary layer and reach the wall. As a result, the droplets will have little influence on cooling the fuel rod surfaces at locations above the quench front where the cladding temperature is in excess of T_{MIN}.

3. Please explain why [

]^{a,c}

Accordingly, an increased heat transfer rate could lead to under predicting the PCT. Such changes in the coding of relations in WCOBRA/TRAC-TF2 that are implemented without providing the underlying technical basis or discussing possible impact on prediction results of safety relevance are found unacceptable. Please explain this specific case and clarify if such an approach has been applied with regard to other constitutive relations coded in WCOBRA/TRAC-TF2. Present a table that documents such deviations in as coded expressions and the actions taken to rectify or substantiate each individual occurrence of such a modification.

4. Please provide plots of WCOBRA/TRAC-TF2 prediction results for the parameters listed below for FLECHT SEASET Tests 31504, 35304, 31805, 34006, 34907, 35807, 34209, 34103, 33903, 31922, and 31108:

   a) forced convective heat transfer coefficient to vapor,
   b) grid enhancement multiplier, F_{grid},
   c) two-phase enhancement multiplier, $F_{2\phi}$
   d) radiation heat transfer coefficient to vapor,
   e) radiation heat transfer coefficient to droplets,

    f)   Forslund-Rohsenow drop-wall direct contact heat transfer coefficient,

    g)   interfacial heat transfer coefficient between the drops and the vapor,

    h)   droplet number and diameter,

    i)   minimum stable film boiling temperature, T_{MIN}.

Plot the above parameters as function of time for the elevation of PCT occurrence and for two additional elevations located approximately two and four feet below the hot spot. In addition, please show the steam and liquid flow rates, void fraction, steam temperature, liquid temperature, and clad temperature as function of time at all three locations. Please plot also a comparison of the measured local PCT against the code predictions as a function of the vertical test bundle axis.

5.   Please provide plots of WCOBRA/TRAC-TF2 prediction results for the following FLECHT low flooding rate skewed power shape tests:

Parametric Effects:	Run Numbers:
Flooding rate (in/sec):	0.6, 0.8, 1.0, 1.5, 3, 6, 15606, 15305; 13404, 13303, 12102, 13001
Pressure (psia): 20, 40, 60	13609, 13404, 13711
Initial Cladding Temp (°F):	500; 1,000; 1,600 12816, 12515, 13303
Subcooling (°F): 5, 80, 140	15713, 13812, 13914
Peak Power (kW/ft): 0.45, 0.7, 1.0	11618, 13303, 16022
Initial (Variable) Flooding Rate:	15305, 15132, 15034

Include plots of the following quantities:

    a)   forced convective heat transfer coefficient to vapor,

    b)   grid enhancement multiplier, F_{grid},

    c)   two-phase enhancement multiplier, $F_{2\phi}$,

    d)   radiation heat transfer coefficient to vapor,

    e)   radiation heat transfer coefficient to droplets,

    f)   Forslund-Rohsenow drop-wall direct contact heat transfer coefficient,

    g)   interfacial heat transfer coefficient between the drops and the vapor,

    h)   droplet number and diameter,

    i)   minimum stable film boiling temperature, T_{MIN}.

Plot the above parameters as function of time for the elevation of PCT occurrence and for two additional elevations located approximately two and four feet below the hot spot. In addition, please show the steam and liquid flow rates, void fraction, steam temperature, liquid temperature, and clad temperature at function of time as all three locations.

Present plots that show the parametric effects with regard to flooding rate, pressure, initial clad temperature, subcooling, peak power, and initial (variable) flooding rate on the WCOBRA/TRAC-TF2 capabilities to predict the FLECHT test data. Please plot also a

comparison of the measured local PCT against the code predictions as a function of the vertical test bundle axial position.

6. The WCOBRA/TRAC heat transfer from the fuel rod to the surrounding media does not consider rod-to-rod thermal radiation. Since the FLECHT and other heat transfer data contain thimbles, cooler neighboring rods, and wall bundle boundaries, etc. that absorb thermal radiation from the hot rod of interest, please explain how the convective heat transfer coefficient is extracted/determined from all test data where thermal radiation is a component heat transfer removal mechanism.

Response:

Part (1)

In WCOBRA/TRAC-TF2, the dispersed flow film boiling (DFFB) wall heat transfer regime is assumed when the void fraction is [

]^{a,c} The dispersed flow film boiling model as documented in WCAP-16996-P [1] is composed of four components, (1) convective heat transfer to vapor, (2) radiation heat transfer to vapor, (3) radiation heat transfer to droplets, and (4) the droplet-wall direct heat transfer. The heat transfer from the wall to vapor is further transferred to liquid droplets through liquid-vapor interfacial heat transfer. The DFFB wall heat transfer mechanism is detailed in Section 7.2.7 of WCAP-16996-P, and the dispersed droplet interfacial heat transfer is described in Section 6.2.7. Following a postulated large break loss-of-coolant accident (LBLOCA), the peak cladding temperature (PCT) typically occurs during the reflood phase of a LBLOCA, so the heat transfer process, which ultimately cools the hottest elevation of the fuel, is characterized by DFFB heat transfer and single phase vapor heat transfer.

Due to the significance of the DFFB heat transfer regime, it has been a consistent challenge to the nuclear thermal hydraulic community to develop a sound DFFB heat transfer model. Extensive experiments have been conducted, and numerous research articles have been published in the last 50 years. However, there still lacks mechanistic models that include an accurate description of all the thermal hydraulic phenomena characterizing the DFFB heat transfer process.

The thermal hydraulic model developed for a LOCA safety evaluation code is restricted by the resolution limit of the computer code, where the core is represented by multiple vertical channels with lateral connections between channels, and the 3-D effects are largely ignored (see Phenomena Identification and Ranking Table (PIRT) discussion on core 3-D effect in Section 2.3.2.2 of WCAP-16996-P). Thus, there is no ideal engineering solution to practically combine the LOCA safety evaluation code with the convoluted fluid flow or heat transfer models.

The DFFB models, as described in WCAP-16996-P, utilize the modified Forslund-Rohsenow correlation to predict the droplet-wall direct heat transfer and the droplet-vapor interfacial heat transfer. Those models are consistent with the corresponding models described in WCAP-12945-P-A [2]. The only update is [

]^{a,c}

Due to the limitation of the original Forslund and Rohsenow experiment and the models modified by Westinghouse to account for the thermal hydraulic condition in a LOCA, an extensive assessment matrix was developed for the DFFB regime. Those tests featured full height, full pressure, and prototypical fuel assemblies. The parameter ranges in the experiments cover the parameter ranges expected in a pressurized water reactor (PWR) LOCA (see the response to Request for Additional Information (RAI) 57). The assessments in Section 15 of WCAP-16996-P show that the DFFB wall heat transfer and interfacial heat transfer models are [

]^{a,c} and the uncertainty of the DFFB model is captured through the validation. The uncertainty in the DFFB model is quantified and is applied to the PWR analysis as described in Section 29.4 of WCAP-16996-P.

The uncertainty evaluation accounts for the potential over-prediction of heat transfer due to the DFFB model by the multipliers that are developed based on comparison of code results to test data. By using the overall heat transfer coefficient (HTC) to develop the multipliers, the effects of differences in local conditions are included. Thus, if the model results in over-predicting the HTC relative to the test data, the multiplier will account for this effect. Furthermore, the [

]^{a,c}

Part (2)

The Forslund-Rohsenow correlation was developed based on the dispersed flow film boiling data with nitrogen as the coolant. The experimental parameters, such as mass flux, heat flux, pressure, exit quality, etc., have been summarized in the RAI. The original Forslund-Rohsenow model was modified by Westinghouse to account for the thermal hydraulic condition in a PWR LOCA, and the modified model was applied to predict droplet-wall contact heat transfer in the DFFB regime as shown by Eq. 7-132 in Section 7.2.7 of WCAP-16996-P. In the modified model, [

]^{a,c}

Due to the limitation of the original Forslund and Rohsenow experiment and the modified model by Westinghouse, the DFFB wall heat transfer model has been validated against various test facilities that are full height and full pressure and have prototypical fuel assemblies as shown in Sections 15.5 and 15.6 of WCAP-16996-P. The assessment matrix on DFFB heat transfer in the blowdown phase is shown in Section 15.5 of WCAP-16996-P. The validation tests [

]^{a,c} The assessments on DFFB heat transfer during the reflood phase are provided by the reflood validation tests in Section 15.6 of WCAP-16996-P, [

]^{a,c} (It is noted that DFFB is not expected during a small break LOCA transient.)

A direct comparison of the parameters ranges in the original Forslund and Rohsenow experiments to the same parameters ranges in the PWR LOCA is not appropriate because the Forslund and Rohsenow experiment was based on a different coolant (nitrogen). The comparison would require

proper dimensionless numbers. For the purpose of a bottom-up review, the adequacy of the model is based on comparing flow conditions considered in the extensive DFFB validation tests, which are full height, full pressure, and with prototypical fuel assemblies, to the expected flow conditions in a PWR LOCA. This comparison is provided in Table 57-6 of the response to RAI 57. [

                    ]^{a,c}

It is worthwhile to note that the experimental study provided by Ghazanari et al. (1980) [4] concludes that at the high flow quality the wall-droplet contribution to the total wall heat transfer is negligible. This appears to be consistent with the expected scenario in a LBLOCA. In the limiting LBLOCA case, due to the low reflooding rate, the flow quality at the upper portion of core is high, and the steam Reynolds number tends to be low. Thus, the contribution of droplet-wall direct contact heat transfer to the overall DFFB heat transfer is small at the typical LBLOCA conditions. Previous sensitivity studies performed to support the licensing of the Code Qualification Document (WCAP-12945-P-A) showed that the Forslund-Rohsenow droplet-wall contact heat transfer (without modification) represents only [   ]^{a,c} of the total heat transfer during DFFB. To demonstrate the contribution in a WCOBRA/TRAC-TF2 calculation, the local wall heat flux near the PCT location of the Beaver Valley Unit 1 LBLOCA double-ended guillotine (DEG) case with a break discharge coefficient (CD) equal to 1.0 is extracted to reveal the contribution of droplet-wall direct contact heat transfer. The ratio of droplet-wall heat transfer to the total wall heat transfer at each time step for the first [   ]^{a,c} of the transient, which is sufficient to cover the PCT time, is calculated and the frequency of the ratios is plotted in a histogram as shown in Figure 56-1. The histogram shows the contribution of the droplet-wall direct contact heat transfer is [

                    ]^{a,c} In general, this study concludes that the contribution of droplet-wall direct contact heat transfer is insignificant compared with the convective and radiation heat transfer to vapor for a limiting LBLOCA case.

Since the predicted contribution of the droplet-wall contact during DFFB is small, it is being removed from the DFFB heat transfer regime model. Therefore, the dispersed flow film boiling model is now composed of three components, (1) convective heat transfer to vapor, (2) radiation heat transfer to vapor, and (3) radiation heat transfer to droplets. This change will be revised accordingly in the updated topical report.

Part (3)

As previously stated, the droplet-wall contact (i.e., the modified Forslund-Rohsenow correlation) is being removed from the DFFB heat transfer regime in WCOBRA/TRAC-TF2. As such, response to this question is no longer necessary.

Parts (4) and (5)

Of the tests listed, FLECHT SEASET 31504 and 31805 and FLECHT SKEWED 15305, 13609, 15713, 13812 and 13914 tests were simulated. In addition, FLECHT SEASET Tests 31203, 31701 and 32013 and FLECHT Low Flooding Rate Tests 04641, 05029 and 05132 were simulated.

Most of the information requested is not readily available (quantities are internally calculated within WCOBRA/TRAC-TF2 and not written to the output files); however, comparison of simulated results to test data are presented in Section 15.0 of WCAP-16996-P which does provide information requested, specifically as follows:

- Section 15.6.1 documents the simulations of FLECHT SEASET Tests 31203, 31504, 31701, 31805 and 32013 and provides comparison plots for:

    o Cladding temperature at several elevations

    o Vapor temperature at several elevations

    o Cladding temperature vs. axial elevation at two transient times near PCT time

    o Predicted PCT versus measured PCT for several thermocouples at various elevations

- Section 15.6.2 documents the simulations of FLECHT Low Flooding Rate Tests 04641, 05029 and 05132 and provides comparison plots similar to the ones provided for the FLECHT SEASET tests.

- Section 15.6.3 documents the simulation of FLECHT SKEWED Tests 13609, 13812, 13914, 15305 and 15713 and provides comparison plots similar to the ones provided for the FLECHT SEASET tests.

- Section 15.9.1 documents predicted versus measured PCT, quench times and PCT turnaround times for the FLECHT tests.

- Section 15.9.2 documents an assessment of the reflood droplet generation for Tests 31701 and 31805.

    o Section 15.9.3 documents a discussion regarding parametric effects due to flooding rate, pressure and subcooling for the FLECHT tests.

In addition to the results presented in Section 15.0, Sections 24.6.4, 24.6.5 and 24.6.6 provide results and discussion in support of the compensating error assessment related to Post-CHF heat transfer for FLECHT SEASET Tests 31504, 31805 and 31701, respectively. Lastly, Section 29.1.8 provides a discussion related to minimum film boiling temperature and predicted versus measured quench temperatures for the reflood tests simulated. It is noted that per Table 29-2 of WCAP-16996-P, the minimum film boiling temperature for the [

]^{a,c}

While all the information requested is not directly contained within the above cited sections of the topical report, the assessment regarding reflood heat transfer (which includes dispersed flow film boiling) is thorough and focuses on the overall behavior of the code during the reflood phase, which includes an assessment related to compensating errors.

It is noted that the comparisons provided in WCAP-16996-P are from the execution of a code version that includes the drop-wall direct contact heat transfer, which is no longer considered a component of the DFFB heat transfer model, as discussed in Part (2) previously. As reported in the response to RAI 77, the [

]a,c, respectively. With the removal of the drop-wall direct contact heat transfer, the

[

]a,c This demonstrates that with the removal of the drop-wall direct contact heat transfer, the overall model is more conservative.

Part (6)

The effect of rod-to-rod radiation heat transfer is addressed in Section 29.4.3.4 of WCAP-16996-P, Volume III. In summary, [

]a,c See Section 29.4.3.4 of WCAP-16996-P for more information.

a,c

Figure 56-1: Contribution of droplet-wall contact heat transfer to the total wall heat transfer near the PCT location of Beaver Valley Unit 1 LBLOCA DEG Case with CD=1.0.

References

1. WCAP-16996-P/WCAP-16996-NP, Volumes I, II and III, "Realistic LOCA Evaluation Methodology Applied to the Full Spectrum of Break Sizes (FULL SPECTRUM LOCA Methodology)," November 2010.

2. WCAP-12945-P-A, Revision 2 (Volume 1) and Revision 1 (Volumes 2 through 5), "Code Qualification Document for Best Estimate LOCA Analysis," March 1998.

3. Removed.

4. Ghazanfari, A., Hicken, E.F., and Ziegler, A., "Unsteady Dispersed Flow Heat Transfer Under Loss-of-Coolant Accident Related Conditions," Nuclear Technology, Vol. 51, pp. 21-26, 1980.

Question #57: Large Break LOCA Heat Transfer Package in WCOBRA/TRAC-TF2

Please provide a summary table that presents the core heat transfer package that is implemented in WCOBRA/TRAC-TF2 and as it is applied in the modeling of LBLOCA transients. Include five columns identifying LBLOCA phases, pre-CHF, CHF, transition boiling, and dispersed flow film boiling correlations. Provide the implemented relations for the three major post-LBLOCA phases blowdown, refill, and reflood with each phase presented by a separate raw in the table. Include the corresponding expressions for each correlation as coded in WCOBRA/TRAC-TF2, the range of applicability of the correlation, and a typical range of flow and heat transfer conditions as occurring in a PWR core following an LBLOCA. Justify the applicability of each model for prototypical reactor core analyses.

Response:

In this response, a summary of the core heat transfer package is presented for each wall heat transfer mode in WCOBRA/TRAC-TF2, in a format not exactly the same as that requested in the RAI question. For each heat transfer mode, its applicability in the applicable phases of the blowdown, refill and reflood phases of a LBLOCA is discussed in addition to other requested information related to the model itself. In doing so, it is an attempt to present the same requested information in a concise and clear format and avoid multiple duplications or cross references of the heat transfer discussion since there are multiple cases that one heat transfer mode is expected to occur and is important in not just one phase of the three phases of a LBLOCA.

In WCOBRA/TRAC-TF2, the vessel heat transfer package consists of a library of heat transfer correlations and the selection logic to determine which correlation is appropriate [

]^{a,c} The heat transfer mode selection logic can be found in Figure 7.2-2 of WCAP-16996-P (referred to herein as the topical report). The following list gives the heat transfer modes used in the WCOBRA/TRAC-TF2 core heat transfer package together with the index of the tables, in which the model description and model correlation range, typical ranges of flow and heat transfer conditions in a PWR LBLOCA, and justifications of the applicability are addressed. There are eight wall heat transfer modes in the core heat transfer package. In addition, the critical heat flux temperature as requested in this RAI is added to the list.

	Wall Heat Transfer Mode	Table Index
Mode 1	Single-phase liquid convection (SPL)	Table 57-1
Mode 2	Subcooled nucleate boiling (SUBC)	Table 57-2
Mode 3	Saturated nucleate boiling (NUCB)	Table 57-2
	Critical Heat Flux (CHF)	Table 57-3
Mode 4	Transition boiling (TRAN)	Table 57-4
Mode 5	Inverted annular film boiling (IAFB)	Table 57-5
Mode 6	Inverted annular dispersed flow (IADF)	Table 57-5

Mode 7   Dispersed droplet film boiling (DFFB)   Table 57-6

Mode 8   Single-phase vapor (SPV)   Table 57-7

Tables 57-1 through 57-7 describe, each wall heat transfer mode respectively, the model correlations, the equation numbers in the topical report, the applicable ranges of the correlation and its references, and the equation numbers of the as coded correlations in the topical report. A discussion on the correlation applicability of the correlation is also presented in each table, together with the typical PWR LBLOCA parameter ranges and the validation test parameter ranges.

The as-coded correlations in topical report (Sec. 7.2.1 through 7.2.8) include the [

]^{a,c} for each wall heat transfer mode, in addition to the model correlations. The as-coded correlation equation numbers as shown in the topical report are listed in Tables 57-1 through 57-7.

Table 57-8 provides a summary table that presents the expected heat transfer modes during the PWR LBLOCA for the blowdown, refill, and reflood phases.

According to the FSLOCA PIRT (Table 2-1 of the topical report), the importance of each wall heat transfer mode in the core heat transfer package is different for the PWR LBLOCA prediction.
[

]^{a,c} The post-CHF wall heat transfer mode include those of the transition boiling, inverted annular film boiling, inverted annular dispersed flow, dispersed droplet film boiling, and single phase vapor. As discussed in Section 14.1 of the topical report, [

]^{a,c}

References

1.   Rohsenow, W.M., et al. Handbook of Heat Transfer, 3rd edition, McGraw-Hill, 1998.

2.   Leung, J.C.M., et al. "Critical Heat Flux Predictions during Blowdown Transients," Int. J. Multiphase Flow, Vol.7, pp. 677-701, 1981

Note: The references to this response include the two listed above and those in the topical report. The same reference style in the topical report is used herein for those references listed in the topical report.

Table 57-1: Single Phase Liquid (SPL) (Note 1)						
Model Description	Topical Report Equation Number	Correlation Range	Correlation Reference	Typical LBLOCA Range in PWR	As-Coded Correlation Equations Numbers in Topical Report	Applicability
Kim's correlation for laminar flow	Equation : 7-1	Laminar Flow Regime	Kim (1979)	[$]^{a,c}$	Equations: 7-1 through 7-7	Note 2,3
Dittus and Boelter correlation for fully developed turbulent flow	Equation : 7-2	Pr: 0.7 ~ 120 Re: 2.5 x 10^3 ~ 1.24x10^5 L/d: > 60	Table 5.11 of Reference 1			

Notes:

1. As one of the heat transfer modes occurring in the covered core, single phase liquid heat transfer is ranked [$]^{a,c}$ (Table 2-1 of the topical report) for all three phases of a LBLOCA.

2. The Dittus and Boelter correlation covers a wide range of turbulent flow conditions measured by the Reynolds and Prandtl numbers. The Kim's laminar flow correlation covers the laminar flows in the low end of the Reynolds number range.

3. [

$]^{a,c}$

Table 57-2: Subcooled Nucleate Boiling (SUBC) / Saturated Nucleate Boiling (NUCB) (Note 1)						
Model Description	Topical Report Equation Number	Correlation Range	Correlation Reference	Typical LBLOCA Range in PWR	As-Coded Correlation Equation Numbers in Topical Report	Applicability
Chen's correlation	NUCB: Equations: 7-8 through 7-15 SUBC: Equations: 7-16 through 7-25	Pressure (psia): 8 ~ 505 Liquid Velocity (ft/s): 0.2~14.7 Quality (%): 1.0~ 71.0 Heat Flux (Btu/hr-ft^2): 1.3x10^4 ~ 7.6x10^5	Chen (1963)	Blowdown Note 2 Reflood [ ]^{a,c}	Equations: 7-26 through 7-48 and 7-19	Note 2,3,4

Notes:

1. Both the subcooled nucleate boiling and saturated nucleate boiling are predicted by the Chen's correlation in WCT-TF2, and are addressed in one table here.

2. The SUBC and NUCB modes [   ]^{a,c} (Table 2-1 of the topical report) for all three phases of a LBLOCA as part of the heat transfer to [

                                                                           ]^{a,c}

3. The Chen flow boiling heat transfer correlation assumes that both nucleation and convective mechanisms occur and it makes the transition to single-phase forced convection at low wall superheat, and to pool boiling at low flow rate. Though it was originally developed for saturated nucleate boiling, existing research by Moles and Shaw (1972) show that it can be applied with satisfactory agreement for low to moderate subcooling.

4. [

5.   ]^{a,c}

For a gravity reflood situation, the inlet flooding rate is oscillatory in nature, due to manometric effects between the core and the downcomer.

Table 57-3: Critical Heat Flux (CHF)

Model Description	Topical Report Equation Number	Correlation Range	Correlation Reference	Typical LBLOCA Range in PWR	As-Coded Correlation Equations Numbers in Topical Report	Applicability	WCT-TF2 Validation Test Range
Modified Zuber's pool boiling CHF	Equation: 7-49	Pressure (atm): 1-10 Subcooling (°C): 5-60 (water, mass flux near zero)	Bjornard and Griffith (1977) Zuber et al. (1961)	Blowdown [	Equations: 7-51 through 7-62	Note 1,2,3	Note 3
Groeneveld CHF look-up table	Not Applicable	Tube Diameter (mm): 3-25 Pressure (MPa): 0.1-21 Mass Flux (kg m^{-2}s^{-1}): 0-8000 Vapor Quality: X_{chf} ~1.0 L/D: >25	Groeneveld (2007)	]^{a,c}			

Notes:

1. The CHF phenomenon is ranked [   ]^{a,c} (Table 2-1 of topical report). [

                                 ]^{a,c} The Groeneveld CHF table was developed based on a large test database covering a wide range of the thermal hydraulic conditions (Groeneveld, 2007). Reference 2 confirms the wide application range of the modified Zuber's pool boiling model.

2. The WCT-TF2 CHF model was assessed against prototypical rod bundle experiments in Section 15.3 of the topical report. The validation tests for LBLOCA include the ORNL dispersed flow film boiling tests and LOFT experiments. [

     ]^{a,c}

3. The pressure range of ORNL dispersed flow film boiling tests reaches 2040psia and the LOFT tests reach the PWR pressure of 2250psia. [

                 ]^{a,c}

Table 57-4: Transition Boiling (TRAN)

Model Description	Topical Report Equation Number	Correlation Range	Correlation Reference	Typical LBLOCA Range in PWR	As-Coded Correlation Equation Numbers in Topical Report	Applicability	WC/T-TF2 Validation Test Range
Maximum of Model 1 and Model 2 as described in Section 7.2.4 of the Topical Report	Equations: 7-63 through 7-72	Note 1	Iloeje et al. (1974) Ganic and Rohsenow (1977) Forslund and Rohsenow (1968) Bjornard and Griffith (1977) Bajorek et al. (1998) Zuber et al. (1961)	Blowdown [ ]^{a,c} Reflood [ ]^{a,c}	Equations: 7-79 through 7-86, 7-72, 7-70, 7-75, 7-76, 7-62, 7-78b, 7-66, 7-52, 7-160, 7-161, and 7-43	Note 2	Prototypical PWR rod bundles Blowdown (Taken from Table 14.1-3 of the Topical Report) [ ]^{a,c} Reflood (Taken from Table 14.1-6 of the Topical Report) [ ]^{a,c}
	Equation: 7-73 through 7-76						
Top-down quench transition boiling model	Equation: 7-77 through 7-78b						

Notes:

1. [

   ]^{a,c} Due to the unstable nature of transition boiling, the TRAN heat transfer mode involves complicated hydrodynamic and heat transfer phenomenon and is modeled with numerous correlations as shown in Sec. 7.2.4 of the topical report.

   [

   ]^{a,c}

2. The validation of the transition boiling mode using WCT-TF2 is part of the overall post-CHF heat transfer validation to evaluate the blowdown rewetting and reflood quenching. Thus the transition boiling heat transfer is assessed against G1 blowdown tests in Section 15.5 of the topical report for the blowdown rewetting and the FLECHT tests in Section 15.6 of the topical report for the reflood quenching. To justify the applicability of the TRAN model in WCT-TF2, the ranges of important parameters of the transition boiling in the validation tests are compared with the typical ranges in PWR. [

   ]^{a,c}

For a gravity reflood situation, the inlet flooding rate is oscillatory in nature, due to manometric effects between the core and the downcomer.

Table 57-5: Inverted Annular Film Boiling (IAFB) / Inverted Annular Dispersed Flow (IADF)							
Model Description	Topical Report Equation Number	Correlation Range	Correlation Reference	Typical LBLOCA Range in PWR	As-Coded Correlation Equation Numbers in Topical Report	Applicability	WC/T-TF2 Validation Test Range
Modified version of the Bromley correlation for IAFB ($\alpha_V <$ [ ]^{a,c})	Equations: 7-92 through 7-95	Geometry: external horizontal tube with F-113 Pressure: Atmospheric $\Delta T(°F)$: 200 ~ 500 Heat Flux (Btu/hr-ft^2): $5 \times 10^3 ~ 2.5 \times 10^4$	Pomerantz (1964)	Reflood [	Equations: 7-96 through 7-107	Note 1	Prototypical PWR rod bundles Reflood (Taken from Table 14.1-6 of the Topical Report) [
IADF is interpolated between IADF and DFFB if [ ]^{a,c}				]^{a,c}	Equations: 7-108 through 7-111		]^{a,c}

Notes:
1. [

]^{a,c} WCT-TF2 extends the application of Pomerantz (1964) correlation to a steam-water system at a higher pressure than atmospheric, and the validation tests for these heat transfer modes aim to compare the quench front progressing between the code prediction and the test data. The IAFB and IADF heat transfer models are validated as part of the overall post-CHF model package that impacts the blowdown and reflood rewetting/quench behavior. Those validation tests are listed in Table 14.1-6 of the topical report. The ranges of important parameters in the validation tests are compared with the typical ranges in PWR. [
]^{a,c}

*For a gravity reflood situation, the inlet flooding rate is oscillatory in nature, due to manometric effects between the core and the downcomer.

Table 57-6: Dispersed Flow Film Boiling (DFFB)

Model Description	Topical Report Equation Number	Correlation Range	Correlation Reference	Typical LBLOCA Range in PWR	As-Coded Correlation Equation Numbers in Topical Report	Applicability	WC/T-TF2 Validation Test Range
The total DFFB heat flux comprises of				Blowdown/Refill			Blowdown/Refill
1. Convective heat flux to vapor including the spacer grid and two phase enhancement	Equations: 7-113, 7-114 and 7-135 through 7-141	Note 1	[$]^{a,c}$ Kays (1966)	Table 14.1-4 of Topical Report Reflood	Equations: 7-142 through 7-153	Note 2,3	Table 14.1-4 of Topical Report Reflood
2. Radiation heat transfer to vapor and droplets	Equations: 7-115 through 7-129	Note 1	Sun, Gonzalez, and Tien, (1976)	Table 14.1-5 of Topical Report			Table 14.1-5 of Topical Report
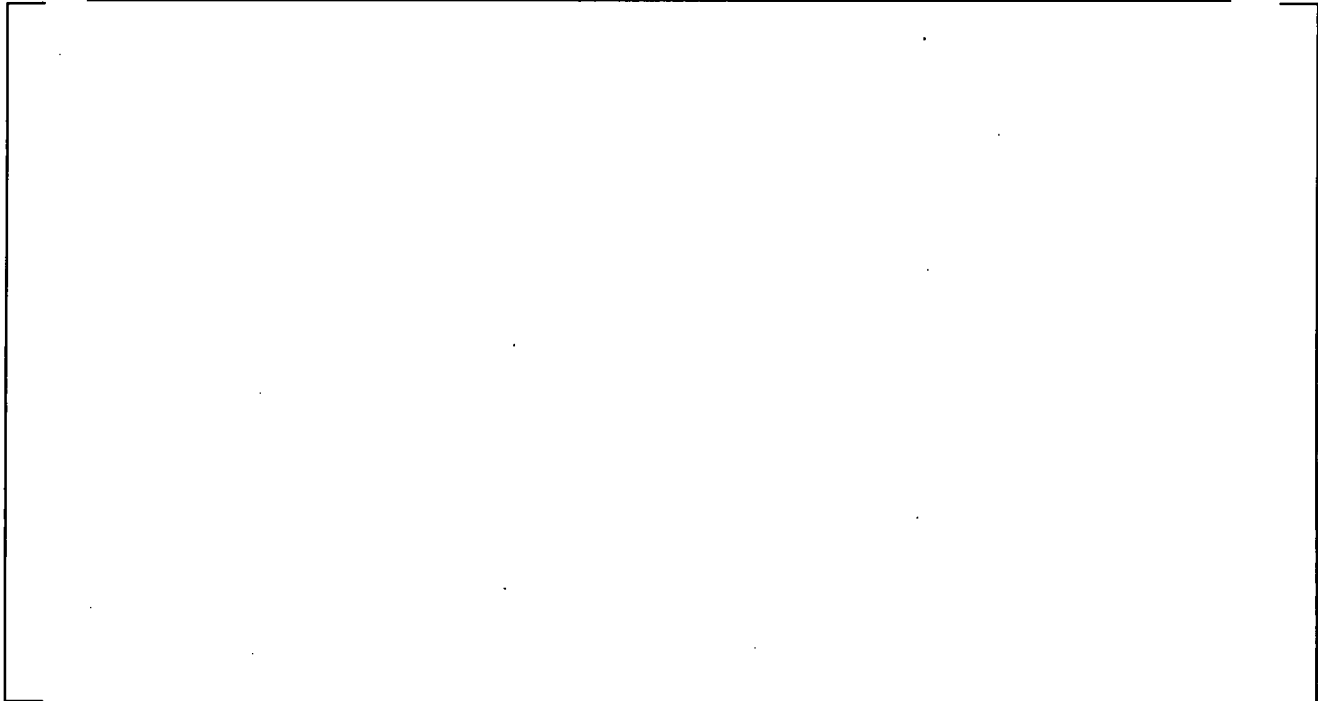
Notes:

1. [$]^{a,c}$ The DFFB heat transfer mode involves complicated hydrodynamic and heat transfer phenomena and is modeled with numerous correlations as shown in Sec. 7.2.7 of the topical report. [

$]^{a,c}$

2. The assessment of DFFB heat transfer in the blowdown phase is shown in Section 15.5 of the topical report. The validation tests (ORNL-THTF high pressure film boiling tests (Section 15.5.2.1), G-1 intermediate pressure blowdown heat transfer tests (Section 15.5.2.2), and G-2 low pressure refill heat transfer tests (Section 15.5.2.3)) indicate that [$]^{a,c}$ The assessments of DFFB heat transfer in reflood phase are provided by multiple reflood validation tests in Section 15.6, including FLECHT SEASET, FLECHT Low Flooding Rate, FLECHT skewed, and G-2 Reflood tests. [
$]^{a,c}$

3. To justify the applicability of the DFFB model in WC/T-TF2, the ranges of important parameters of DFFB in the validation tests are compared with the typical ranges in PWR. [

$]^{a,c}$

Table 57-7: Single Phase Vapor (SPV)							
Model Description	Topical Report Equation Number	Correlation Range	Correlation Reference	Typical LBLOCA Range in PWR	As-Coded Correlation Equation Numbers in Topical Report	Applicability	WC/T-TF2 Validation Test Range
McAdams correlation for turbulent free convection	Equation:7-154	Ra: $10^9 \sim 10^{13}$ Re: < 2000	McAdams (1954)	Table 14.1-2 of the Topical Report	Equations: 7-160 through 7-166	Note 1	Table 14.1-2 of the Topical Report
Lee's Laminar forced convection heat transfer model	Equation: 7-157	Laminar flow regime	Lee (1981)				
Wong and Hochreiter forced turbulent heat transfer correlation	Equation: 7-159	Re: $2.5 \times 10^3 - 2.52 \times 10^4$ Pressure (psia): 20-60	Wong and Hochreiter (1981)				

Notes:

1. [$]^{a,c}$ The Nusselt number in the laminar
   forced convection is suggested by Lee (1981) based on the rod bundle tests. [
                                        $]^{a,c}$ The Wong and Hochreiter (1981) correlation is similar to the Dittus-Boelter
   correlation, but the coefficients are generated by fitting the steam cooling heat transfer data in a 17X17 rod bundle at the reflood-type pressure.
2. The assessment on SPV heat transfer is shown in Section 15.4 of the topical report. The validation tests include the ORNL-THTF uncovered bundle
   heat transfer tests and the FLECHT SEASET SPV tests and the SPV heat transfer coefficients and wall temperatures in the tests [
                      $]^{a,c}$ Table 14.1-2 of the topical report shows that [

                                                                    $]^{a,c}$

Table 57-8: Generally Expected Heat Transfer Modes During the Major LBLOCA Transient Phases

a,c

Question #58: Flow Regime Map Selection Criterion for Vessel Component

The mixture level swell in the reactor core governs the fuel cladding temperature response in the late stages of a small or intermediate break LOCA when the reactor core can uncover. The WCOBRA/TRAC-TF2 vessel component relies on flow regime maps in modeling the two-phase flow behavior including the response of the reactor core region. WCAP-16996-P/WCAP-16996-NP, Volumes I, II, and III, Revision 0, Section 4, "WCOBRA/TRAC-TF2 Flow Regime Maps and Interfacial Area," explains that the code vessel component utilizes two different flow regime maps: (1) a "Normal Wall" or also referred to as a "Cold Wall" flow regime map and (2) a "Hot Wall" flow regime map. The former is applied when a momentum cell contains heated surfaces that are expected to be fully wetted by liquid and the latter is used to describe the hydrodynamics of highly non-homogeneous and thermally non-equilibrium two-phase flow that can take place during blowdown and reflood. Subsection 4.2, "Vessel Component Normal Wall Flow Regimes," explains that the criterion for selecting a flow regime map, defined by Equation (4-1), is based on the surface temperature of the heated structures present within a computational cell. As described in Subsection 4.2, the transitional temperature is set equal to "the surface temperature at the critical heat flux," T_{CHF}, approximated as $T_w = T_{CHF} \approx (T_{sat}+75)$ °F = $(T_{sat}+41.7)$ K and limited by the critical water temperature given as 705.3 °F (374.1 °C or 647.2 K). When the metal surface temperature exceeds the CHF criterion, it is assumed that the liquid can only partially wet the wall and the "Hot Wall" flow regime map is used. Below T_{CHF}, it is considered that the liquid fully wets the wall and the "Cold Wall" flow regime map is applied.

The "Cold Wall" flow regime map recognizes four different regimes: (1) SB with a flow regime indicator ISIJ of 1 (see Table 4.2-1, "Summary of Flow Regime Number in Vessel Components"), (2) SLB with ISIJ=2, (3) CT, and (4) FD with ISIJ=5. The "Hot Wall" flow regime map identifies five individual regimes: (1) Subcooled Inverted Annular, (2) Inverted Liquid Slug, (3) Dispersed Droplet, (4) Falling Film, and (5) Top Deluge with ISIJ=11. The selection of the vessel flow regime takes place in subroutine INTFR, which also computes the wall and interfacial drag coefficients.

(1) Please explain the appropriateness and provide the technical basis in support of the implemented criterion in Equation (4-1) for selection between the "Cold Wall" and the "Hot Wall" flow regime maps in two-phase flow modeling for the vessel component. Clarify if the WCOBRA/TRAC-TF2 applies the same modeling approach to both plant designs with top down cooling (i.e., Upper Plenum Injection (UPI) plants) and bottom up re-flood. As different validation/qualification processes apply to both designs, please describe the technical bases that demonstrate the applicability of the modeling 'approach for each plant design.

(2) As explained in Subsection 4.2, "It is assumed that for cells in which a metal surface temperature exceeds the criterion given by Equation (4-1), liquid can only partially wet the wall and the hot wall flow regime is used." The introduced phenomenological approach for flow regime map selection between the "Cold Wall" map and the "Hot Wall" map is based on surface wetting. At the same time, when surfaces are hot enough, liquid droplets are not

expected to even partially wet the metal wall. Please clarify how the phenomenon of hot surface wetting relates to the flow map identification criterion defined by Equation (4-1).

(3) Please explain which heat transfer correlations are employed in WCOBRA/TRAC-TF2 to model partially wetted wall surfaces and describe the applicable technical basis. In particular, identify and describe the data used to validate the wetting of walls and related heat transfer when the wall surface temperature, T_w, is above the defined criterion for wall surface wetting.

(4) Please explain how the criterion defined by Equation (4-1) and the assumed approximation for the CHF surface temperature as $T_{CHF} \approx (T_{sat}+75)$ °F relate to the Leidenfrost wall temperature limit, T_{Leid}. A simple correlation for the Leidenfrost temperature used by Bricard et al. (see Bricard, P., Péturaud, P. and Delhaye, J. M., "Understanding and Modeling DNB in Forced Convective Boiling: Modelling of a Mechanism Based on Nucleation Site Dryout," Multiphase Science and Technology, No. 9, p. 329, 1997) gives $T_{Leid}=(T_{sat}+150)$ °C. Similarly, a range of Leidenfrost wall superheat of 100 to 150 °C is provided by Celata et al. (see Celata, G. P., Cumo, M., Mariani, A. and Zummo, G., "Burnout in subcooled boiling of water. A visual experimental study," Int. J. Therm. Sci., No. 39, pp. 896-908, 2000).

Response:

The $T_{CHF} \approx T_{SAT} + 75$°F criterion was originally implemented in Westinghouse Best-Estimate LBLOCA evaluation models [1,2,3]. This criterion was found to provide reasonable agreement with well-accepted correlations and experimental data under LBLOCA reflood conditions.

Carbajo (Carbajo, J., 1985 [4]) noted that the most significant contributor to T_{CHF} was the pressure. He compared T_{CHF} to various correlations and experimental data as a function of pressure. This comparison is presented as Figure 1, with the addition of the $T_{CHF} \approx T_{SAT} + 75$°F criterion.

It is observed that for pressures less than 0.5 MPa (73 psia): T_{SAT} + 75°F, Thom, Weatherhead, Jens and Lottes, and the experimental data are all in good agreement. At higher pressures which are more representative of SBLOCA conditions, T_{SAT} + 75°F tends to fall in between the correlations and the experimental data.

The value of T_{CHF} for selection of the flow regime is expected to be less significant under SBLOCA conditions. Given the interface between the two-phase level and single-phase vapor, the cladding will heatup, and the flow regime will switch from cold wall to hot wall at the point where the transition to single phase vapor occurs (Figure 2). As such, application of Equation 4-1 is also judged to be acceptable for SBLOCA conditions.

Sensitivity studies were executed with ROSA Test SB-CL-02 and a Beaver Valley PWR SBLOCA case with TCHF = T_{SAT} + 150°F to illustrate the lack of sensitivity. The ROSA study results are presented in Figures 3 through 7. The red, solid lines are Equation 4-1 from WCAP-16996-P, and the green, dashed lines are with TCHF = T_{SAT} + 150°F. It is observed that the

[

]^{a,c} The Beaver Valley PWR study results are presented
in Figures 8 through 13. The red, solid lines are Equation 4-1 from WCAP-16996-P, and the
green, dashed lines are with TCHF = T_{SAT} + 150°F. Again it is noted that [

]^{a,c}

It is therefore concluded that based on the comparisons to data, correlations, and the sensitivity
study described previously that the vessel flow regime selection is appropriate.

Supplemental Discussion Specific to Question 58, Part 1

The same models are used in <u>W</u>COBRA/TRAC-TF2 for plants equipped with Upper Plenum
Injection (UPI) as for non-UPI plants. This was the same approach used for prior best-estimate
LBLOCA evaluation models. It is important to note that under LBLOCA transient conditions
even plants equipped with UPI experience a bottom-up reflood rather than top-down cooling.
The UPI water tends to preferentially drain through the low power assemblies, and then refill the
core from the bottom (see Section 5-4-3-5 of WCAP-14449-P-A, Revision 1). The UPI is not of
consequence for SBLOCA since the high head safety injection is into the cold legs for 2-loop
Westinghouse-designed plants, and the reactor coolant system (RCS) pressure is above the
low head safety injection cut-in pressure during the period of interest for the transient.

Supplemental Discussion Specific to Question 58, Part 3

[

]^{a,c}

**Supplemental Discussion Specific to Question 58, Part 4**

There is no direct relationship between the criterion in Equation 4-1 of WCAP-16996-P and the
Leidenfrost temperature. The Leidenfrost temperature is generally compared to the minimum
film boiling temperature. It is expected that the critical heat flux temperature would be less than
the Leidenfrost temperature (e.g. Equation 1 from Carbajo, J., 1985), which is the case given
the discussion in the papers cited in the RAI.

References

1) WCAP-12945-P-A, Volume1, Revision 2, Volumes 2 through 5, Revision 1, "Code
   Qualification Document for Best Estimate LOCA Analysis," March 1998.

2) WCAP-14449-P-A, Revision 1, "Application of Best Estimate Large Break LOCA
   Methodology to Westinghouse PWRs With Upper Plenum Injection," October 1999.

3) WCAP-16009-P-A, "Realistic Large-Break LOCA Evaluation Methodology Using the Automated Statistical Treatment Of Uncertainty Method (ASTRUM)," January 2005.

4) Carbajo, Juan J., "A Study on the Rewetting Temperature," *Nuclear Engineering and Design*, Vol. 84, pp. 21-52, 1985.

5) WCAP-16996-P, "Realistic LOCA Evaluation Methodology Applied to the Full Spectrum of Break Sizes (FULL SPECTRUM LOCA Methodology)," November 2010.
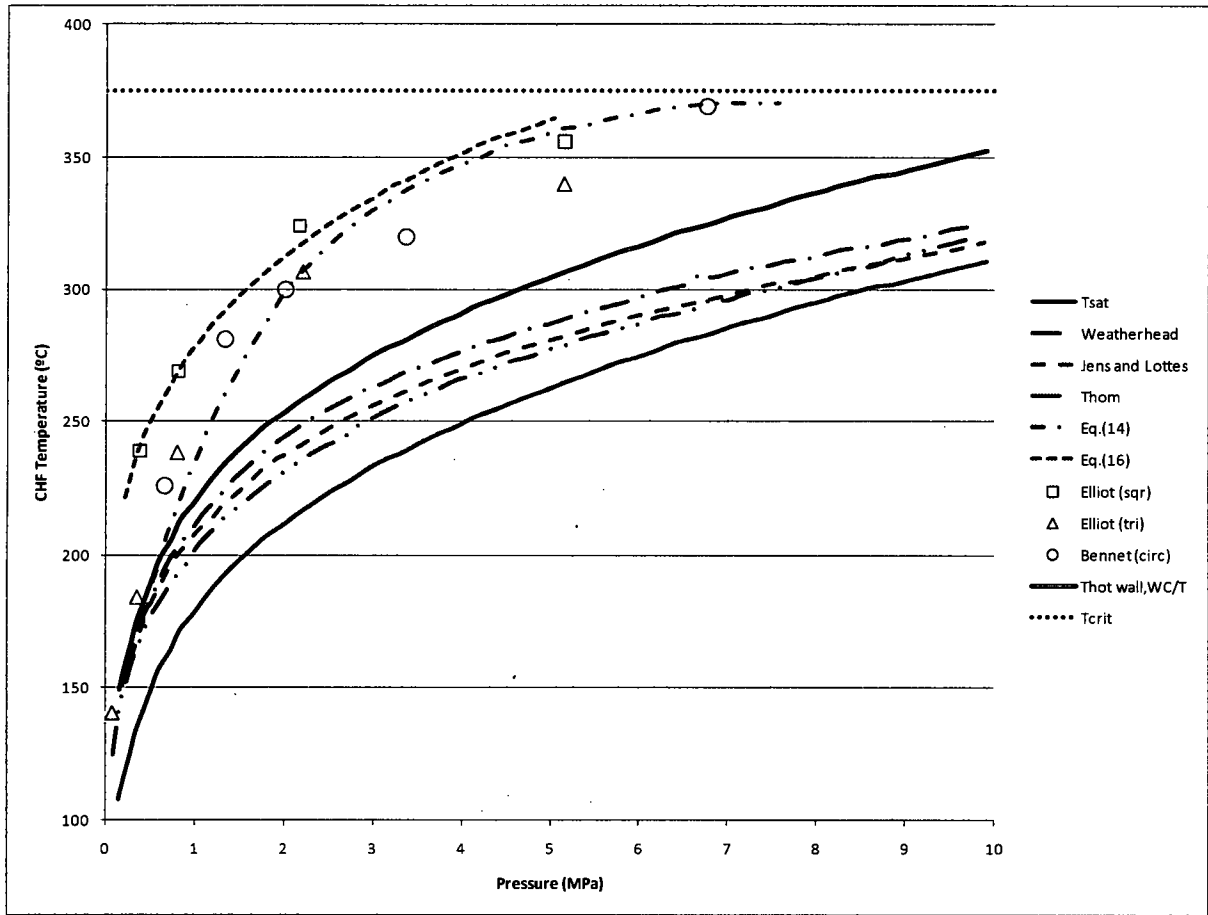
Figure 1: Comparison of WCOBRA/TRAC-TF2 T_{CHF} Criterion with Various Correlations and Experimental Data

a,c

Figure 2: Comparison of the Heat Transfer Mode and Cladding Temperature for the Simulation of G2 Test 715
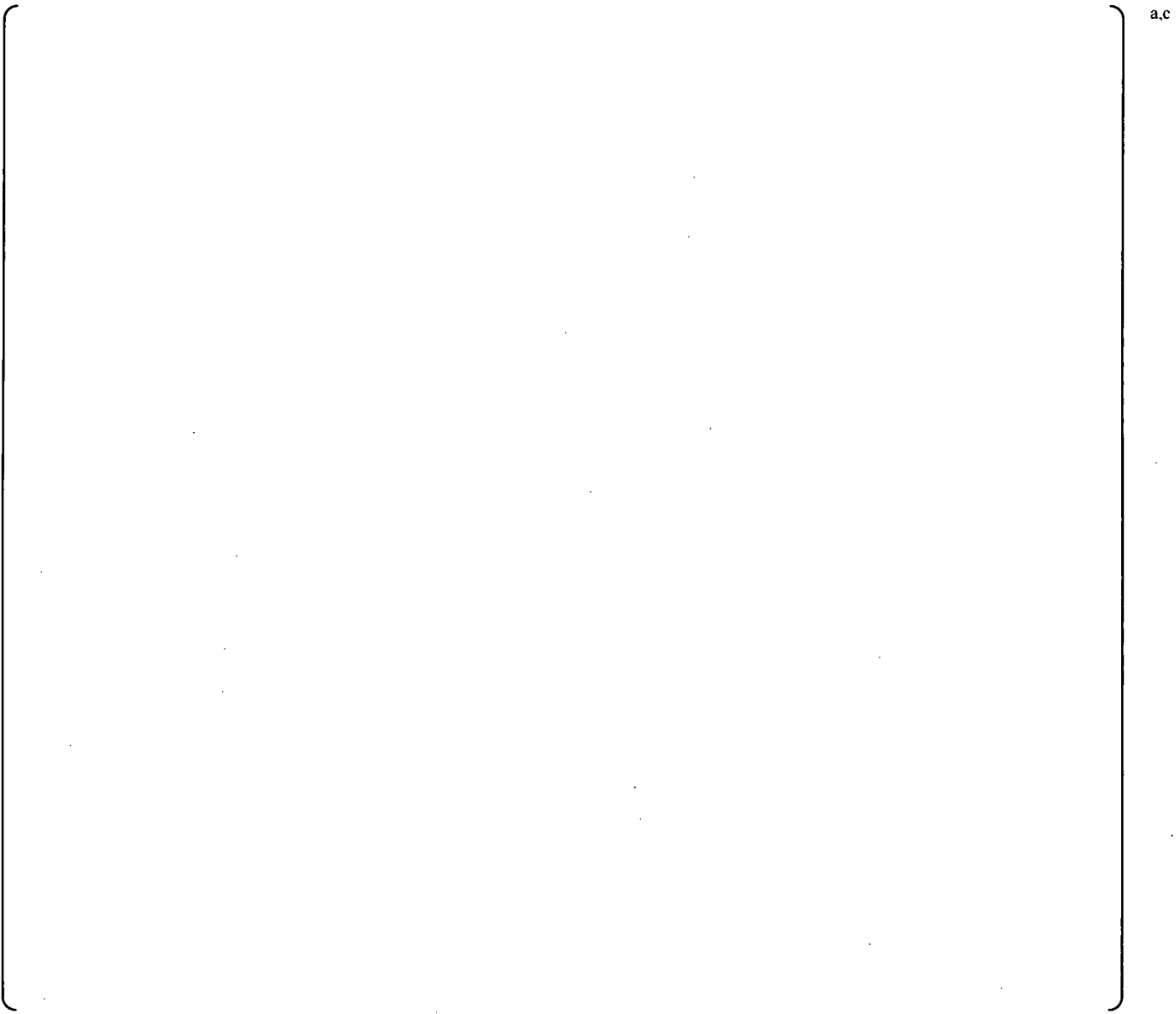
a,c

Figure 3: Pressurizer Pressure for the ROSA SB-CL-02 Critical Heat Flux Temperature Sensitivity

a,c

Figure 4: Vessel Fluid Inventory for the ROSA SB-CL-02 Critical Heat Flux Temperature Sensitivity

a,c

Figure 5: Cladding Temperature at the 6-foot Elevation for the ROSA SB-CL-02 Critical Heat Flux
Temperature Sensitivity

c

a,c

Figure 6: Cladding Temperature at the 8-foot Elevation for the ROSA SB-CL-02 Critical Heat Flux Temperature Sensitivity

a,c

Figure 7: Cladding Temperature at the 10-foot Elevation for the ROSA SB-CL-02 Critical Heat Flux Temperature Sensitivity

a,c

Figure 8: Pressurizer Pressure for the Beaver Valley Unit 1 PWR Critical Heat Flux Temperature Sensitivity

a,c

Figure 9: Vessel Fluid Inventory for the Beaver Valley Unit 1 PWR Critical Heat Flux
Temperature Sensitivity

a,c

Figure 10: Cladding Temperature at the 8-foot Elevation for the Beaver Valley Unit 1 PWR Critical Heat Flux Temperature Sensitivity

a,c

Figure 11: Cladding Temperature at the 9-foot Elevation for the Beaver Valley Unit 1 PWR Critical Heat Flux Temperature Sensitivity

a,c

Figure 12: Cladding Temperature at the 10-foot Elevation for the Beaver Valley Unit 1 PWR Critical Heat Flux Temperature Sensitivity

a,c

Figure 13: Cladding Temperature at the 11-foot Elevation for the Beaver Valley Unit 1 PWR Critical Heat Flux Temperature Sensitivity

Question #75: Interfacial Drag Sampling Impact on ROSA-IV LSTF Test Predictions

WCAP-16996-P/WCAP-16996-NP, Volumes I, II, and III, Revision 0, Section 29, "Assessment of Uncertainty Elements," identifies the bubbly flow drag multiplier, YDRAG, as a parameter that describes model uncertainties related to "thermal-hydraulic global models." YDRAG, described in WCAP-16996-P/WCAP-16996-NP, Volumes I, II, and III, Revision 0, Subsection 29.1.5 as being "applied directly to the small bubble, large bubble and hot wall interfacial drag calculations," is characterized by [   ]^{a,c} According to Table 29-2, "Uncertainty Elements – Thermal-Hydraulic Models," it has [
                    ]^{a,c}

WCAP-16996-P/WCAP-16996-NP, Volumes I, II, and III, Revision 0, Section 13, "Core Void Distribution and Mixture Level Swell," assesses WCOBRA/TRAC-TF2 interfacial drag and level swell prediction capabilities using SET data. An additional interfacial drag study is presented in WCAP-16996-P/WCAP-16996-NP, Volumes I, II, and III, Revision 0, Subsection 21.15, "YDRAG Sensitivity Calculations," also comparing code predictions against test data from an IET performed at the LSTF as part of the Rig-of-Safety Assessment No. 4 (ROSA-IV) Program. The effect of YDRAG variation for the core channels on transient calculations was analyzed and results compared against data for ROSA-IV LSTF Test SB CL-18 simulating a 5 percent cold leg break. The YDRAG multiplier in the core region was set [
]^{a,c} and the sensitivity results are presented in Figures 21.15-1 through 21.15-6. The difference in the PCT predictions following core boiloff amounts to approximately 100° F (55.6 K) according to Figure 21.15-6, "Peak Cladding Temperatures." This ROSA-IV reference transient, Test SB-CL-18, is first analyzed in Subsection 21.4, "Simulation of SB-CL-18, 5-Percent Cold Leg Side Break," [   ]^{a,c} in the core region. According to WCAP-16996-P/WCAP-16996-NP, Volumes I, II, and III, Revision 0, Subsection 21.3, this YDRAG value was used for all analyses presented in WCAP-16996-P/WCAP-16996-NP, Volumes I, II, and III, Revision 0, Section 21, "ROSA IV Test Simulations," except for the YDRAG sensitivity studies for Test SB-CL-18 discussed in Subsection 21.15. As explained in Subsection 29.1.5, [

                    ]^{a,c}

In assessing code compensating error, Subsection 24.8, "Core Level Prediction in SB-CL-18 Test," presents Figure 24.8.3-2, "Impact of YDRAG Variation on Predicted Level Swell," showing level swell predictions obtained with YDRAG values [   ]^{a,c} for Test SB CL-18 and with YDRAG values [   ]^{a,c} for Test SB-CL-01 (2.5 percent cold leg break) against the estimates from test measurements.

(1)   Please provide two additional assessments for ROSA-IV LSTF Test SB-CL-18 using the YDRAG sampling range upper limiting value of [   ]^{a,c} and its model nominal value of 1.0. Provide comparisons of WCOBRA/TRAC TF2 predictions against measured data including clad temperature measurements at deferent axial elevations. Include comparisons for the axial void

distribution in the core at the time of PCT occurrence as well as for the collapsed liquid level and two-phase mixture level as functions of time. Document the predicted maximum PCT values following core boiloff and compare them against the measured PCT value including the measurement accuracy as well.

(2)   Please analyze and provide code predictions for ROSA-IV LSTF Test SB CL-01 (2.5 percent cold leg side break), Test SB-CL-02 (2.5 percent cold leg bottom break), and Test SB CL-03 (2.5 percent cold leg top break). In all three experiments, the measured PCTs reached a maximum value of approximately 1,205°F (925 K). In addition to the results obtained for these tests with [   ]^{a,c} and presented in Subsection 21.7, please provide code predictions for YDRAG drag multipliers [   ]^{a,c} and compare code results against test data. Include also comparisons for the axial void distribution in the core at the time of PCT occurrence as well as for the collapsed liquid level and two-phase mixture level as functions of time.

Response:

The question appears to address the apparent inconsistency between the established range of YDRAG uncertainty, [   ]^{a,c} per Section 29.1.5 of [1], and the range of YDRAG sensitivities performed with the ROSA-IV LSTF 5% CL break test SB-CL-18 and the 2.5% CL break tests SB-CL-01, SB-CL-02 and SB-CL-03.

It is important to note that, while selected tests at the ROSA-IV LSTF integral test facility were used to validate the code capability to model the system response (overall and phenomenon specific), there is no specific intent to use the ROSA tests to establish uncertainty of separate effect phenomena; for example level swell, which is affected by the YDRAG multiplier. The YDRAG sensitivities with the ROSA test SB-CL-18, Section 21.15 of [1], were used to confirm that the code calculation response to the YDRAG variations are consistent with the expectations in terms of effect and direction of bias.

Furthermore, the YDRAG sensitivity calculations with the ROSA 5% break test SB-CL-18 reported in Section 21.15 of [1] bound the new reduced YDRAG uncertainty range [
]^{a,c} proposed in the response to RAI #74. Therefore, based on the revised range of YDRAG, and the YDRAG sensitivities with the ROSA test SB-CL-18 the requested analyses are not necessary.

References

1. **WCAP-16996-P, Volumes I through III**, "Realistic LOCA Evaluation Methodology Applied to the Full Spectrum of Break Sizes (FULL SPECTRUM LOCA Methodology)," November 2010.

Question #77: Follow-up to RAI #45

[

]^{a,c}

Table 1: Parameters Treated as Sampled Variables in FSLOCA Calculations for RAI 77 Response

[

]^{a,c}

Table 1: Parameters Treated as Sampled Variables in FSLOCA Calculations for RAI 77 Response

[

]a,c

Table 1: Parameters Treated as Sampled Variables in FSLOCA Calculations for RAI 77 Response

[

]^{a,c}

Table 1: Parameters Treated as Sampled Variables in FSLOCA Calculations for RAI 77 Response

[

]^{a,c}

Table 1: Parameters Treated as Sampled Variables in FSLOCA Calculations for RAI 77 Response

[

$]^{a,c}$

Table 2: Parameters Treated as Bounded in FSLOCA Calculations for RAI 77 Response			
Acronym	PIRT	Physical Description	Modeling Approach (How Bounded)

[

]^{a,c}

Table 2: Parameters Treated as Bounded in FSLOCA Calculations for RAI 77 Response			
Acronym	PIRT	Physical Description	Modeling Approach (How Bounded)

[

]^{a,c}

Table 2: Parameters Treated as Bounded in FSLOCA Calculations for RAI 77 Response			
Acronym	PIRT	Physical Description	Modeling Approach (How Bounded)

[

]a,c